Keynote Lecture
Proc. 4th International Conference on Soft Soil Engineering, Vancouver, Canada, October 4-6, 2006, pp. 3-34

STABILITY ANALYSIS ACCOUNTING FOR MACROSCOPIC AND MICROSCOPIC STRUCTURES IN CLAYS

K.Y. Lo, Professor Emeritus and Director, Geotechnical Research Centre, Faculty of Engineering, The University of Western Ontario, London, Ontario, Canada, N6A 5B9
S.D. Hinchberger, Assistant Professor and Research Director, Geotechnical Research Centre, Faculty of Engineering, The University of Western Ontario, London, Ontario, Canada, N6A 5B9

ABSTRACT
Geotechnical Engineering has advanced to the present stage that various types of earth structures can be designed and constructed safely and economically in most instances. However, in some cases, difficulty arises either in the form of failure during construction or after many years in existence. The soils in which these problems occur include but are not limited to highly sensitive clays and stiff fissured clays of various geological origins. These clays possess pronounced macroscopic and microscopic structures that control the strength and deformation properties. Macroscopic structures are visible features that include fissures, joints, stratifications and other discontinuities in an otherwise intact soil mass. Microscopic structures would include soil fabric and cementation bonds. A typical soft clay deposit usually is composed of a weathered crust at the top that is fissured and thus macroscopic structures are dominant and soft clay at depth in which microscopic structures are significant. The properties of these clays are complex, having a stress-strain relationship that exhibits a peak strength and a post peak decrease in strength, a non-linear failure envelope, strength anisotropy and a significant decrease in strength with a slower rate of testing or longer time to failure.

This paper explores implications of microscopic and macroscopic structure on stability problems and the conditions under which difficulties arise. Results of laboratory and field tests together with case histories show that the dominant effect of a macroscopic structure is exhibited in the reduction of undrained and drained strength with the sample size. The mass strength, whether in the undrained or drained condition, is only a fraction of the intact strength. Design analysis for stability conditions should therefore start with the mass strength at initial time followed by a reduction in strength as time progresses. A case history of an embankment founded on stiff fissured clay on which it failed after 32 years is analyzed in detail to illustrate progressive development of plastic zones with construction details and time. The effect of cementation bonds in influencing the strength properties of soft clays is studied by artificially deposited bonds using the electro-kinetic process and examination with the electronic microscope. It is shown that in addition to the classical increase in strength with decrease in water content, a strength increase due to the deposition of cementation bonds with time by diffusion occurred. An important bonding agent is identified and its effect on bond strength is compared with bonding in natural clays. As the height of an embankment founded on a sensitive clay deposit is increased, a plastic zone will develop and increase in size. The pore pressures at a point will increase at a greater rate when the point is engulfed by the plastic zone as a result of bond breakage. Concurrently, the strength will drop to the post-peak state. Case histories of embankments on these clays are analyzed to illustrate the propagation of the plastic zone in controlling the foundation behaviour at imminent instability. The difference in performance of embankments with different geometries in the same clay deposit is investigated. It is shown that the stability and subsequent strength changes are controlled by the extent of the plastic zone. Finally, design considerations are suggested to accommodate the effects of the macroscopic and microscopic structures in these clays.

1. INTRODUCTION

At present, soft clay engineering has advanced to the stage that earth structures can be designed economically and constructed safely in most cases. There are, however, circumstances in which failure has occurred during construction or after many years in existence in spite of the detailed field and laboratory investigations that had been carried out. The soils in which these problems occurred include but are not limited to stiff fissured clays and highly sensitive clays, as exemplified by the following two well-documented case records.

The first case involved an embankment constructed at Nanticoke, Ontario, on a deposit of stiff fissured clay after extensive field and laboratory investigations. The embankment was originally designed for a maximum height of 17m (locally) with 2:1 slopes. It was constructed in 1969 as a containment dyke for fly ash disposal. Surficial instability occurred at various periods after construction with time to failure of several months to several years. The downstream slope was flattened in 1977 to 2.75:1. However, instability occurred at 32 years after construction.

The second case involved a dramatic and most instructive case record presented by Crawford et al. (1995) who described two consecutive failures of an embankment on soft clay, in spite of the fact that two test embankments were already constructed on either side of the failures and that the test embankments were higher than the embankments that failed.

Table 1. Properties of some clays

Site	LL	PI	LI	Undrained Strength (kPa)	Sensitivity	References
Nanticoke	55	31	0.06	380	1	Lo et al. (1969)
Wallaceburg (depth 4.2 m)	46	18	1.0	37	6	Becker (1981)
Sarnia Till	38	26	0.16	150	2	Quigley and Ogunbadejo(1976)
St. Vallier	60	37	0.97	43	20	La Rochelle and Lefebvre (1970)
St. Louis	50	23	1.83	43	50	La Rochelle and Lefebvre (1970)
St. Alban	50	23	2.4	11	14	La Rochelle et al. (1974)
Olga	60	32	1.6	10	13	Dascal et al. (1972)
Vernon	65	40	1.14	30	4	Crawford et al. (1995)

The conditions under which these problems occurred are explored in this paper. Additional considerations to conventional design methodology are suggested.

2. BEHAVIOUR OF INTACT CLAYS

Highly sensitive clays and stiff fissured clays of various geological origins possess pronounced macroscopic and microscopic structures that control the strength and deformation properties.

Macroscopic structures are visible features that include fissures, joints, stratifications and other discontinuities in an otherwise intact soil mass. Microscopic structures would include soil fabric and cementation bonds identifiable, for example, using electron microscope techniques. A typical soft clay deposit usually is composed of a weathered crust at the top that is fissured and thus macroscopic structures are dominant and soft clay below the crust wherein microscopic structures are significant.

The properties of these clays are complex, having a stress-strain relationship that exhibits a peak strength and a post peak decrease in strength, a non-linear failure envelope, strength anisotropy and a significant decrease in strength with a slower rate of testing or longer time to failure. Leroueil (2005) has presented a comprehensive review of the behaviour of sensitive clays. The following discussion covers the behaviour of relatively insensitive intact stiff clays, and a few additional observations are also made on the behaviour of sensitive clays. In order to avoid the effects of sample disturbance, only results of tests from specimens trimmed from block samples or high quality large diameter samples are considered.

2.1 Non-Linearity of Mohr-Coulomb Envelope

Traditionally, engineers have adopted a linear relationship for the Mohr-Coulomb failure envelope. In reality, test results have invariably shown that the envelope is intrinsically nonlinear. However, the details of nonlinearity are markedly different between highly sensitive and relatively insensitive clays. Properties of the clays discussed in the following paragraphs are shown in Table 1.

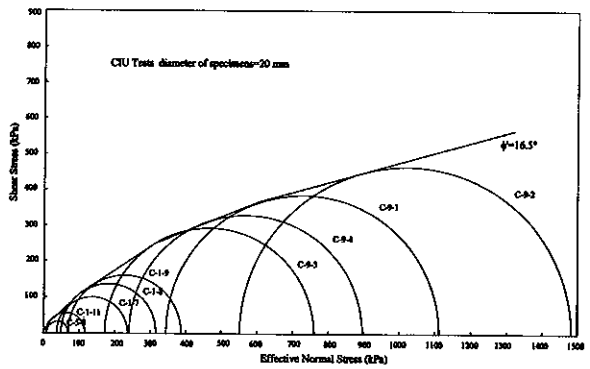

Figure 1. Effective strength envelope of Nanticoke Clay from 4.5 m depth

Figure 1 shows the Mohr-Coulomb envelope determined from intact specimens trimmed from block samples of insensitive stiff fissured clay taken at the Nanticoke Generation Station, Ontario (Vallée 1969). It can be seen that the envelope is mildly nonlinear over a wide stress range with strength increasing with effective stresses. This behaviour is also exhibited in other materials such as intact rock and concrete.

Figure 2 shows the results of tests on Wallaceburg Clay (Becker 1981) near Sarnia, Ontario. The clay is firm at the depth of testing with a liquidity index of about one and a sensitivity of six by field vane tests. It can be seen that the envelope is nonlinear. However, over the stress range from 70 kPa to 90 kPa straddling the preconsolidation pressure, there is little increase in strength with increasing effective stress.

Figure 3 shows the results of CIU tests on St. Louis Clay (S_t=50) (Lo and Morin 1972). The envelope is strongly nonlinear. The remarkable feature is that there is a significant decrease in strength with an increase in effective stress as the consolidation pressure approaches the preconsolidation pressure. Similar behaviour can be seen for St. Vallier Clay (S_t=20) in Figure 4.

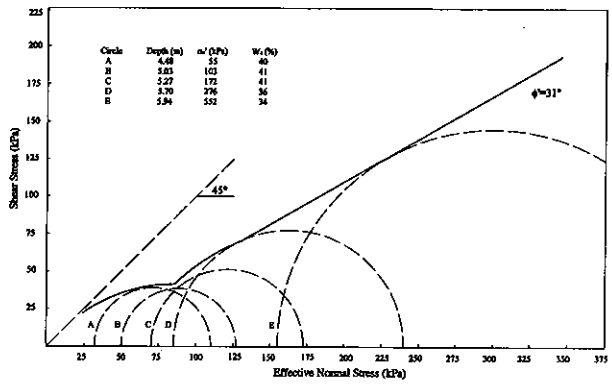

Figure 2. Effective strength envelope of firm Wallaceburg Clay (after Becker 1981)

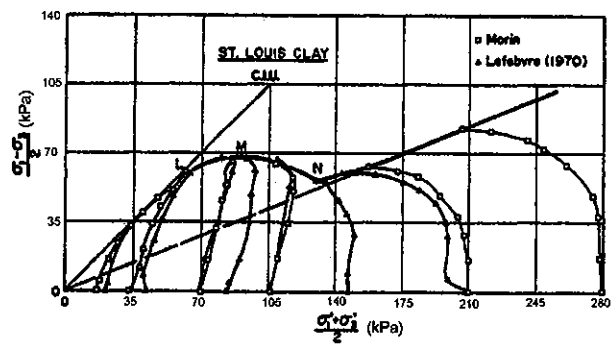

Figure 3. Stress condition at failure and stress paths, CIU tests at i=0 on St. Louis Clay (after Lo and Morin 1972)

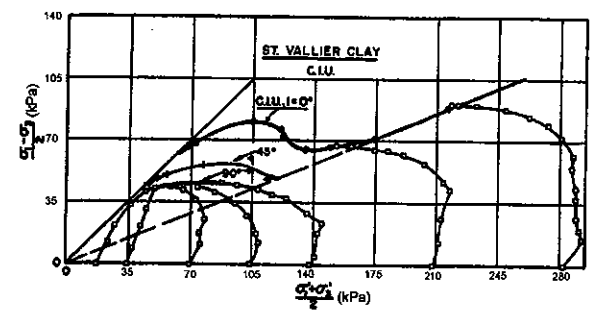

Figure 4. Results of CIU tests at different i on St. Vallier Clay (after Lo and Morin 1972)

2.2 Anisotropy

The results of triaxial compression tests on specimens from St. Vallier with their axes trimmed at 45° and 90° from the vertical are shown in Figure 4. The apparent anisotropy of the strength envelope is evident although the trend of decreasing strength with an increase in effective stress is less distinct. The decrease in strength with an increase in effective stress may be attributed to the bond breakage, a progressive process of damage to the microscopic soil structure in which the strength loss due to bond breakage overshadows the strength gain due to effective stress increases until most of the bonds are broken, whereupon their effects are obliterated. At higher effective stress over the preconsolidation pressure, the envelope enters into the "unstructured" portion where the strength increases linearly with effective stress. Further study of cementation bonds will be discussed in Section 5.

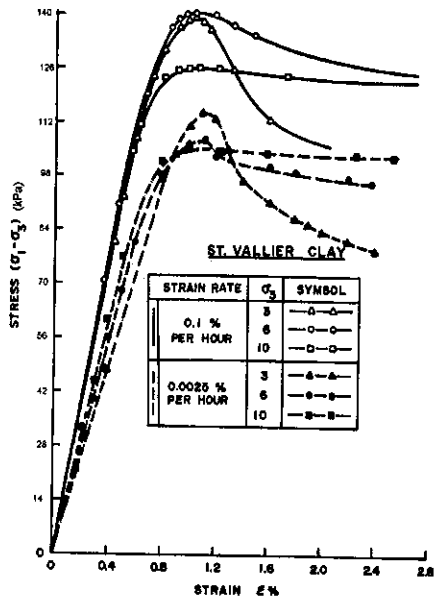

Figure 5. Stress-strain relationship of St. Vallier Clay from drained triaxial tests (after Lo 1972)

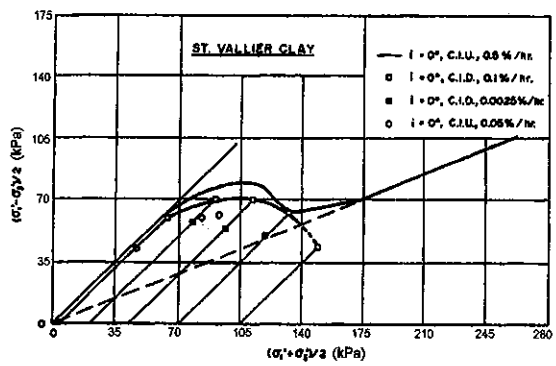

Figure 6. Effect of strain rate on peak strength of St. Vallier Clay (after Lo and Morin 1972)

2.3 Effect of Time

The stress-strain relationship of specimens from block samples of St. Vallier Clay measured in isotropically consolidated drained triaxial tests at consolidation pressures below the vertical preconsolidation pressure are shown in Figure 5 (Lo 1972). One series of tests was

performed at the conventional rate of 0.1% per hour while the other series was performed 40 times slower. It may be seen that both strength and stiffness decreased with the slower rate of testing. The dependence of the failure envelope on the time rate of testing, including CIU tests, are shown in Figure 6 (Lo and Morin 1972). Since the strain rates of laboratory tests are vastly different from the strain rates in the field, the results of these tests indicate that the effect of time to failure is a significant factor to be considered in the design of earth structures.

2.4 Post-Peak Envelope

It has often been found that in most natural soils, the strength decreases after the peak strength has been reached. For sensitive clays, it was recognized that an envelope defined by the state of stresses at strains in the order of 6% to 10% is of particular engineering significance for the analysis of slope stability (Lefebvre and La Rochelle 1974, Lo and Morin 1972). It was considered that the effect of anisotropy, time rate and the potential for progressive failure all tend to reduce the peak strength envelope towards the post-peak strength as shown in Figure 7 (for details see Lo and Morin 1972). Analyses of natural slope failures in Champlain Clays showed that the results lie close to the post-peak envelope as shown in Figure 8 (Lo and Lee 1974). For first time slides of cut slopes, the results lie above the post-peak envelope (see points for Orleans (Lo 1972), Lachute 1 and Lachute 2 (Lefebvre 1981)) as expected, since the progression of progressive failure can satisfy the limiting equilibrium condition before the post-peak strength is reached over the entire slip surface.

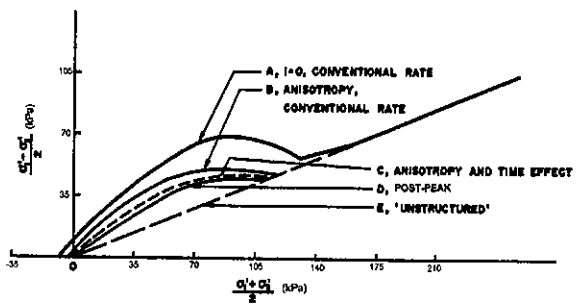

Figure 7. Influence of different physical factors on stress conditions at failure in sensitive clays (after Lo and Morin 1972)

An important contribution to the verification of the concept of the post-peak strength was made by Law (1981). A comprehensive series of tests on specimens prepared from 100 mm Osterberg samples from Rockcliffe in the Ottawa region was performed using different stress paths. The results showed that:

(a) The brittleness of both a sensitive clay and a stiff clay decreases from a constant σ_3' test to constant p' test to constant σ_1' test. However, the brittleness of both clays is still manifested (see Figure 9).

(b) The post-peak envelope is independent of the stress paths and is remarkably similar to that deduced by Lo and Lee (1974) (see Figure 10).

It appears, therefore, that the concept of post-peak envelope remains valid since its inception as a basis for the evaluation of the stability problem.

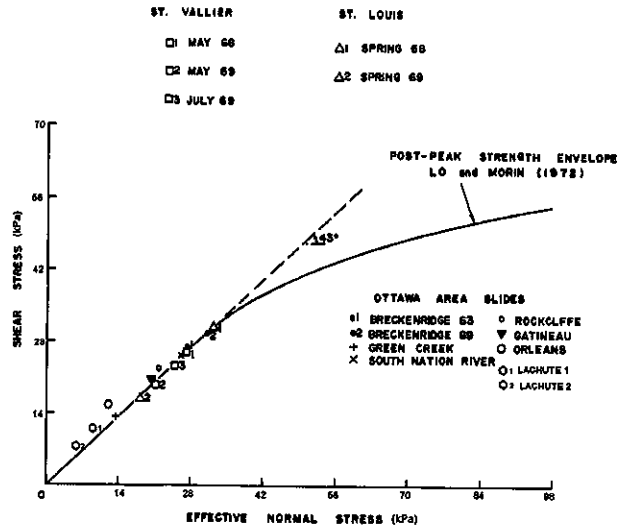

Figure 8. Summary plot for natural slope failures in Champlain Sea Clay (after Lo and Lee 1974, with additional cases)

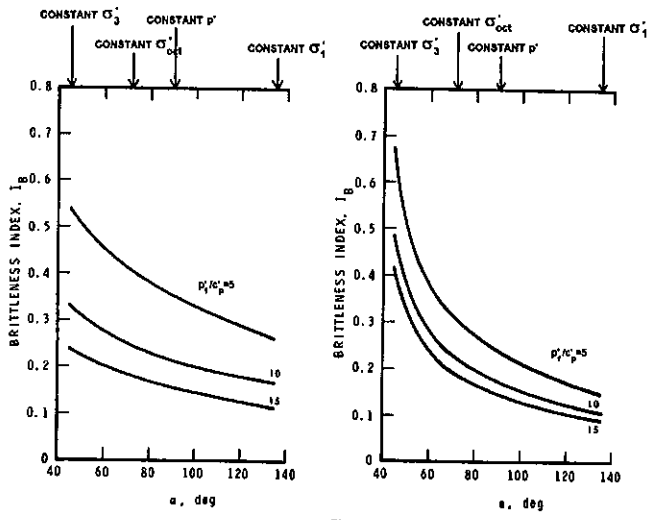

(a) Brown London Clay (b) Rockcliffe Clay

Figure 9. Effect of stress path on brittleness index of clays (after Law 1981)

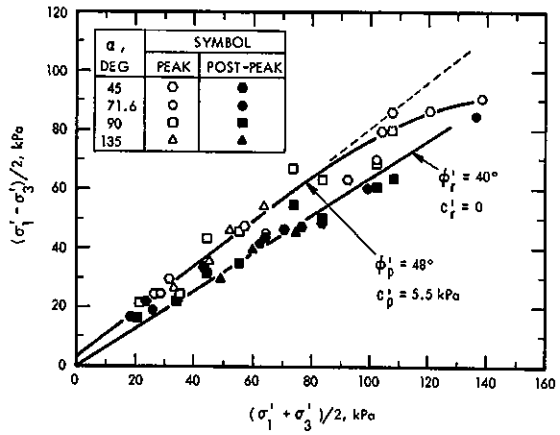

Figure 10. Summary of results of stress path tests on Rockcliffe Clay (after Law 1981)

3. THE MASS STRENGTH OF FISSURED CLAYS

In soil deposits that are essentially free of discontinuities, properties of intact specimens measured in the laboratory would be representative of field behaviour, apart from accounting for their complex behaviour. In a soil mass populated by features such as fissures and joints, properties measured in small "intact" specimens in conventional sampling and testing can be misleading.

It has been recognized that the macroscopic structures of a clay can dominate its strength behaviour and that the strength in the mass is only a fraction of that of the intact material (e.g. Bishop and Little 1967, Lo 1970). Macroscopic structures include fissures, joints and other discontinuities in an otherwise intact soil mass. For comparison, the effective stress parameters of some stiff clays in the intact state, along natural surfaces of weakness, and in the residual state are given in Table 2. It may be seen that the strength along the discontinuities is much lower than the intact material but distinctly higher than the residual strength.

Many hypotheses for the mechanisms of formation of discontinuities in clays have been put forward that include but are not limited to:

(a) weathering: one of the generally accepted mechanisms, including cycles of deposition, desiccation, erosion and redeposition;
(b) syneresis: the colloidal process in which particles are drawn together, forming honeycomb patterns of cracking during aging;
(c) one-dimensional swelling due to removal of overburden such that the strain required to reach passive failure is attained (Skempton 1961);
(d) tectonic stresses;
(e) stress relief and valley rebound due to erosion;
(f) slumps on steep rock valleys during deposition, forming large scale discontinuities;
(g) glacial shear;
(h) temperature effects.

While joints, shear zones and faults affect the directional stability of an earth structure, the most ubiquitous discontinuities are fissures prevalent in stiff fissured clays and the crust of soft or firm clay deposits.

An example of the large difference in undrained strength between fissures and intact material of Nanticoke Clay is shown in Figure 11. Because of the large difference in strength, whether in the undrained (Figure 11) or drained (Table 2) condition, the presence of fissures considerably weakens the otherwise intact soil mass. The degree of weakening would depend on the difference between the intact strength and fissure strength as well as the density and size distribution of the fissures. An example of a decrease in strength with sample size (area of potential failure surface) is shown in Figure 12.

The impact of macroscopic structures on the stability of earth structures such as cut slopes is substantial. Table 3 summarizes some case histories of failure in stiff fissured clays. The quantities S_u and $S_{u,m}$ represent the strengths from conventional unconsolidated undrained tests and the mass strength from back analysis of failure, respectively. F_u is the factor of safety computed from conventional U-U strength. It can be seen that these conventional factors of safety considerably exceed one. It follows, therefore that a design approach without consideration of macroscopic structure could be unsafe.

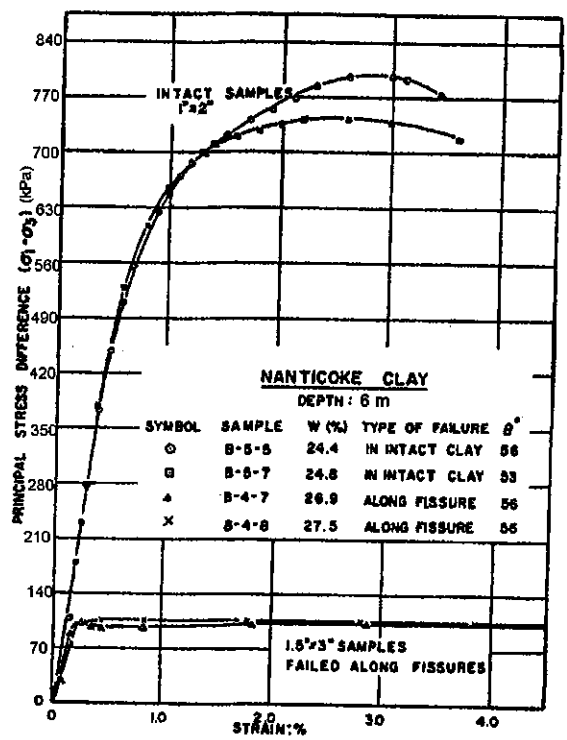

Figure 11. Stress-strain relation of intact and fissure samples-unconsolidated-undrained tests (after Lo 1970)

Table 2. Strength of clays along discontinuities

Clay	Index Properties W_L %	W_P %	W_N %	Type of Discontinuities	Strength Parameters: Intact Material c' kPa	Intact Material ϕ' (°)	Discontinuities c'_w kPa	Discontinuities ϕ'_w (°)	Residual c'_r kPa	Residual ϕ'_r (°)	Reference
Nanticoke Clay Ontario	58	24	26	Fissure (depth=6 m)	31	36	13	18	7	15	Lo & Vallée (1970)
Upper Siwalik Clay Sukian	60	28	16	Minor Shear	58	22	17	16	0	14	Skempton and Petley (1967)
Blue London Clay Wraysbury	70	27	28	Joint and Fissure	31	20	7	18.5	1	16	Skempton et al. (1969)
Barton Clay Hampshire	83	32	30	Fissure	26	38	6	18	3	13	Marsland & Butler (1967) and Corbett (1967)
Magho District Northern Ireland Shale	-	-	-	Bedding Joint	8	25	6	18	5	8	Prior and Fordham (1974)

Table 3. Some case records of failure on fissured clays and rock

Case Record	Soil Type	Structure	W_L (%)	W_P (%)	W_N (%)	LI	S_u kPa	F_u	$S_{u,m}$ kPa	Reference
Bradwell 1 (England)	Brown London Clay	Cut	95	30	33	0.05	97	1.8	54	Skempton and La Rochelle (1965)
Bradwell 2 (England)	Brown London Clay	Cut	95	30	33	0.05	97	1.9	50	
Wravsbury (England)	Blue London Clay	Cut	73	28	28	0.0	118	3.3	36	Simons (1967)
Durgapur (India)	Blue Silty Clay	Cut	58	20	23.4	0.09	113	8.7	13	Dastidar (1967)
Dunvegan (Alberta)	Clay Shale	Fill	50	24	22	-0.08	217	2.6	83	Hardy et al. (1962)
South Saskatchewan	Clay Shale	Cut	80-150	18-27	19-35	--	70	2.5	28	Peterson et al. (1960)
Witbank Colliery (South Africa)	Coal	Pillar	--	--	--	--	31 900	7.4	4300	Bieniawski (1968)
Houston (Texas)	Fissured Clay	Anchored Sheet Pile Wall	65	22	22	0	97-217*	2.2	24-97	Daniel & Olson (1982)

Note: LI = Liquidity Index; S_u = Undrained Strength from Conventional UU tests; F_u = Factor of Safety used on S_u
$S_{u,m}$ = Mass Strength Computed from Failure
* = Increases with depth

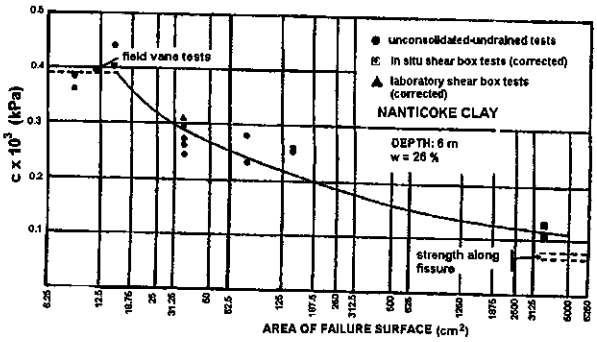

Figure 12. Strength-size relation, Nanticoke Clay from 6 m depth (after Lo 1970)

4. UNDRAINED STRENGTH OF THE CRUSTS OF SOFT CLAY DEPOSITS

It is often found in soft or firm clay deposits that a stiffer crust exists of one to several metres thick. The crust is typically fissured with high vane strength. The strength decreases through the transition zone and from there to the soft layer where the strength increases again (see, for example, Figure 28). The assumption of the value of undrained strength for the crust has a significant effect on the design factor of safety for embankments on soft clays.

The field vane test is commonly used for the measurement of undrained strength in field investigations. However, the failure surface is cylindrical in the field vane test while fissures are approximately planar. Therefore, the likelihood of containing fissures in the vane test is small and the vane test measures essentially the intact strength (Lo 1970) apart from disturbance during insertion and effects of strength anisotropy. The effect of macroscopic structure therefore would require the field vane strength to be reduced to correspond to the mass strength of the crust. Field results of crust mass strength are scarce but the work of Quigley and Ogunbadego (1976) and Lefebvre et al. (1987) are discussed below.

4.1 Sarnia Till

In a comprehensive study of the properties of Sarnia Till in connection with pollutant migration in a Sarnia landfill site, Quigley and Ogunbadejo (1976) performed large *in situ* shear box tests on the Sarnia Till using the same equipment and similar procedure as Lo et al. (1969). The tests were performed at three depths of 1.5, 3.0 and 4.5 metres. The first two levels correspond to the crust and the third level corresponds to the transition zone. The results, shown in Table 4, indicated that the ratio of mass strength to intact strength increases with depth, reflecting the decreasing intensity of fissuring with depth. It is also interesting to note that there is very little post-peak drop in strength for this clay from the *in situ* shear box test with the brittleness index being about 0.07.

4.2 Olga Embankment

An embankment was loaded to failure at the Olga site, in Mattagami, in Quebec (Dascal et al. 1972). The factor of safety computed was 1.6. Trak et al. (1976) re-analyzed the failure using the concept of undrained post-peak strength. However, because of the uncertainty of the crust strength, an investigation was carried out in the crust by Lefebvre et al. (1987). *In situ* shear box tests and plate loading tests were performed in the 1.2m thick crust but no tests were done in the transition zone which extended to about 3 m depth. A large number of vane strength profiles were performed both in two test trenchs (east and north) and there was substantial variability of vane strength. The results of *in situ* shear box tests, however, were quite consistent. The ratio of undrained strength from *in situ* shear box tests to field vane strength was about one quarter and is shown in Table 4.

Table 4. Effect of fissures on the intact undrained strength of clays

Soil Deposit	**Depth (m)**	**S_{ui} (kPa)**	**$S_{u,m}$ (kPa)**	$\frac{S_{u,m}}{S_{ui}}$
Sarnia Till	1.5 (Crust)	280	55	0.20
	3.0 (Crust)	250	104	0.41
	4.5 (Transition)	150	85	0.56
Olga Sensitive Clay	0.2-1.2 (Crust)	75 ($\pm$ 25)	18	0.24 (east trench)
		80 ($\pm$ 40)	18	0.23 (north trench)
Nanticoke G.S.	3.3	333	56	0.17
Fissured Clay	4.8	390	95	0.24
	6.1	371	97	0.26
Brown London Clay, Maldon	1.4-2.0	77	31	0.40

Note: S_{ui} = "intact" undrained strength from UU tests or vane test
$S_{u,m}$ = undrained mass strength from *in situ* shear box tests

4.3 Observations on Mass Strength of Crusts

It is apparent from the results of the *in situ* tests described in the preceding paragraphs and the study on stiff fissured clays at Nanticoke (Lo et al. 1969) and at Maldon (Bishop and Little 1967; also shown in Table 4) that the macroscopic structure of fissuring could reduce the mass strength to about one quarter to one third that of the intact material; the value would depend on the intensity of fissuring at a particular site. As a guideline, the vane strength in the crust of a soft clay deposit should conceivably be reduced to this range.

It is of interest to note that in the planning and execution of the Gloucester Embankment at the National Test Site near Ottawa, the impact of the crust of the sensitive clay was recognized by Dr. M.M. Bozozuk (Bozozuk and Leonards 1972) and it was removed prior to the construction of the test embankment.

5. MICROSCOPIC STRUCTURE

5.1 Conceptual View of Microstructure

Investigations into the microscopic structures of soils have been carried out by numerous authors (see e.g. Mitchell 1976, Rosenquist 1966). As early as 1966, Quigley and Thompson (1966) using the X-ray diffraction technique showed that for a block sample of Leda Clay, soil fabric underwent a large change once the preconsolidation pressure as determined in an oedometer test was exceeded. It was hypothesized that cementation bonding was predominantly destroyed at yield and greater anisotropic loading led to an increased parallel arrangement of clay particles in the oedometer tests. More recently, Leroueil and Vaughan (1990) reviewed the strength behaviour of many natural soils and weak rocks and considered that the effects of structure (microstructure) on engineering behaviour should be treated as a basic concept in geotechnical engineering.

A conceptual view of the microstructure of clays is shown in Figure 13. The structure, consisting of the fabric and the cementation bonds, was developed during and after deposition of the soil under a field stress system and physico-chemical environment. The fabric of sensitive clays may be conceived as a highly complex space frame and derives its resistance to shear by displacements and deformations of its constituent members and joints. The cementation bonds at the contacts of clay platelets are randomly distributed, and are brittle in behaviour requiring little deformation to rupture. For a given physico-chemical system, the relative contribution of the bonds and fabric to the overall mobilized resistance of the soil to deformation would predominantly depend on the intensity and strength of the cementation bonds.

Starting from an equilibrium state, an increase in applied stresses will be transmitted through the soil skeleton (fabric) producing the deformations arising from (a) the elastic deformation of the soil skeleton, (b) deformation and sliding at points of contact, and (c) deformation of the soil particles. Component (c) may be neglected since the compressibility of the soil skeleton is orders of magnitude greater than that of the soil particles. The vectoral summation of these microscopic deformations are observed as strain in a given direction.

As the applied stresses are increased, the external stresses are transferred to the points of contact. Since there is a lack of symmetry in the fabric and the distribution of bonds, the distribution of normal and shear forces at the contact points is not uniform. In addition, distortion of the soil fabric would induce tensile stress in some contact points. The criteria of rupture, whether in shear or in tension, will be satisfied at some contact points leading to bond breakage. The failure at points of contact leads to some particle re-arrangement (see Figure 13), observed externally as plastic (irrecoverable) deformation. The stresses originally carried at the contact points will partly be transferred to the pore water, increasing the pore pressure and partly to the neighbouring points of contact. The shearing resistance of the broken contacts would reduce to that similar to the post-peak strength of the clay. Therefore, even at external stresses well below macroscopic failure of a test specimen, bond breakage occurs and produces some plastic deformation and slight re-arrangement of soil fabric as shown in Figure 13.

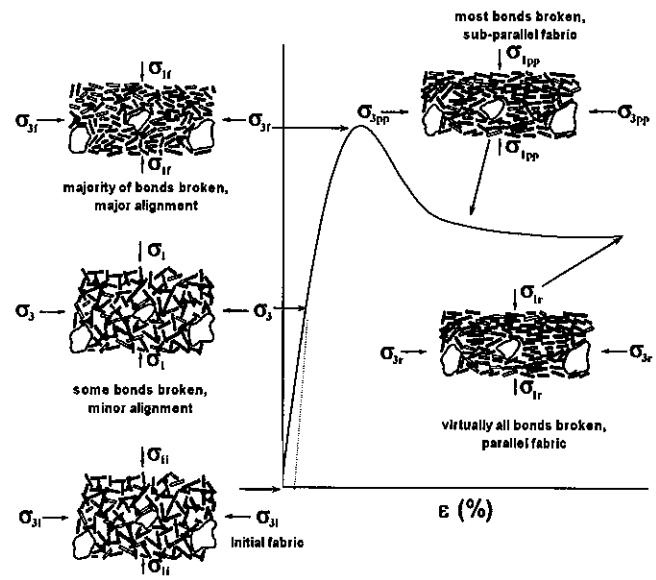

Figure 13. Conceptual view of change of microstructure with shearing in sensitive clays

This process was well illustrated by incremental stress-controlled CIU tests on normally-consolidated sensitive clays in which both plastic deformation (creep) and pore pressure at a constant applied stress increased simultaneously with time (Lo 1961). The progressive

nature of bond rupture during shear can also be illustrated by Figure 14 in which the modulus of deformation of St. Louis Clay in CIU and CID tests are plotted against consolidation pressure. It can be seen that at half of the failure stress, the trend of modulus variation with consolidation pressure reflects that of the curved strength envelope shown in Figure 3.

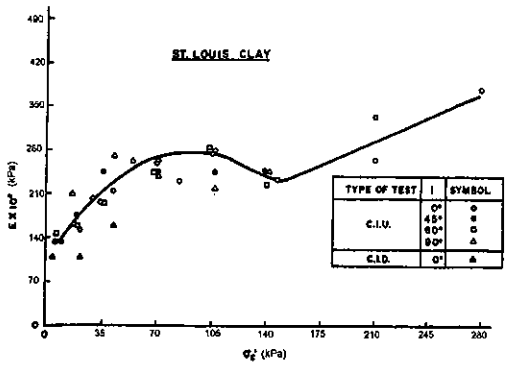

Figure 14. Variation of modulus of deformation with consolidation pressure for St. Louis Clay (after Lo and Morin 1972)

As the applied stress increases in a triaxial test towards the peak stress, localization of deformation occurs due to the formation of a failure zone. Within the failure zone at peak stress, the bond strength is fully mobilized. The test specimen then "softens" and exhibits a decrease in strength with further strain (more correctly, further displacement in the failure zone). The post-peak strength is reached at a moderate nominal strain in the range of 6%-10% in sensitive clays. However, particle parallelism can only be approached at much larger displacement in the region of the residual strength in natural clays.

5.2 Laboratory Study of Cementation Bonds

Studies on the source and nature of cementation bonds in sensitive clays in Eastern Canada have been undertaken by Kenny et al. (1967), Yong et al. (1979) and Quigley (1980), among others. While there was some difference of opinion regarding the details of the methods of these mineralogical and geochemical investigations, there appears to be a general agreement that calcium carbonate and amorphous materials including SiO_2, Fe_2O_3 and Al_2O_3 are the most likely cementing agents in these sensitive clays.

To proceed from qualitative to more quantitative assessment of the contribution of cementation bonds to the overall shear strength of soft clays, one difficulty is the lack of baseline reference for natural clays. It seems appropriate therefore to artificially induce cementation bonds by employing only one potential cementation agent in natural clays, using an untreated sample as a control test throughout the long duration of experimentation, so that their contribution to strength can be ascertained and the possible mechanism of bonding identified.

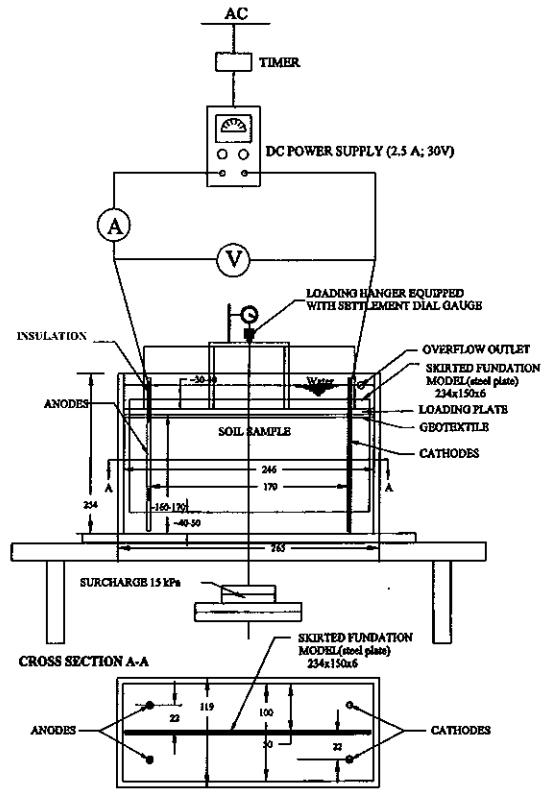

Figure 15. Experimental apparatus (All dimensions in mm; not to scale).

5.3 Artificial Bonding by Electrokinetic Process

Following the discussion in the preceding section, the contribution of cementation bonds to the strength behaviour of soft clays will firstly be examined using artificial bonding achieved by electrokinetic processes. The bonding agent will be iron compounds derived from the iron electrodes during the treatment.

The soft clay used in the experiment is a marine clay from Yulchon, South Korea. The liquid limit of the clay is 59%, plasticity index is 27%, and water content ranges from 80% to 110%. The clay is normally consolidated. The undrained shear strength is between 1 and 6 kPa.

Briefly, the test procedure involves the following steps:

(i) Establish the classical relationship of the undrained shear strength and water content for normally-consolidated clays.

(ii) Set up two identical clay samples under the same pressure and boundary conditions. One sample acts as the control test.

(iii) Treat electrokinetically (EK) the test sample at the applied voltage of 6.2 V using the direct current for seven days, after consolidation at 15 kPa.

(iv) Allow the test to continue for diffusion to take place for a further 45 days after EK treatment.

The test set-up for EK treatment of the Yulchon Clay is shown in Figure 15. Details of the test procedure have been presented in Micic et al. (2002).

Tests were performed before and after the electrokinetic treatment to investigate the changes in the physical, mechanical and chemical properties of the Yulchon Clay due to electrokinetic treatment. The testing program included undrained shear strength and water content measurements, soil chemistry analyses (x-ray fluorescence or XRF, specific surface and cation exchange capacity) and soil surface analyses using a scanning electron microscope (SEM) including energy dispersive x-ray (EDX) analyses for identification of elemental composition of the soil. Based on the results of the tests, the contribution of cementation bonds to the strength behaviour of the Yulchon Clay was evaluated.

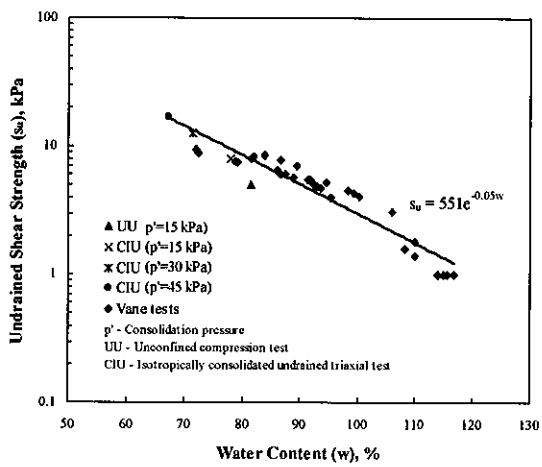

Figure 16. Undrained shear strength of untreated Yulchon soil versus water content

5.4 Results of Artificially-Induced Bonding

Analyses of the relationship between the undrained shear strength and water content of the normally-consolidated (7-15 days of consolidation) Yulchon Clay show that the undrained shear strength and water content of Yulchon soil yield an exponential relationship as shown in Figure 16. Results of isotropically-consolidated undrained triaxial (CIU) tests shown in Figure 17 indicate the ratio s_u/p_c' of 0.3, where p' is the consolidation pressure. This value is similar to the *in situ* value of $s_u/p' = 0.26$ at the Yulchon site in South Korea reported by Hyundai Engineering and Construction Co. Ltd. (HDEC) in 1996. As expected, the stress-strain curves in Figure 17 showed no post-peak decrease in strength.

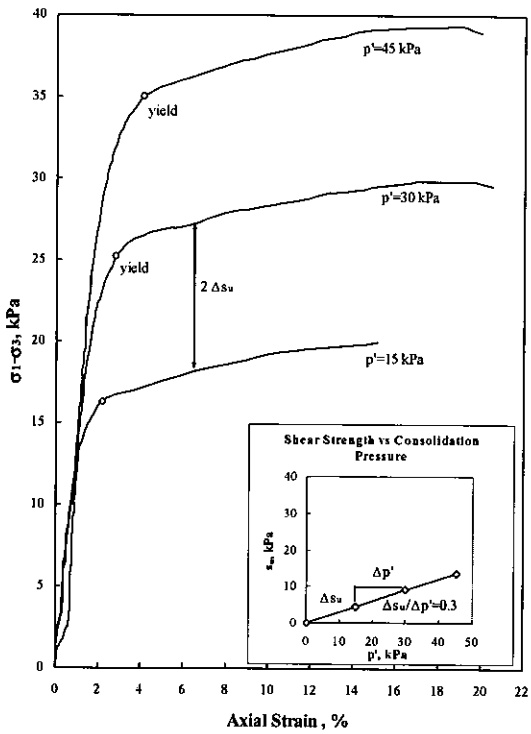

Figure 17. Results of CIU triaxial tests on natural Yulchon Clay

The results of undrained shear strength changes after EK treatment of the Yulchon Clay are shown in Figures 18. Figures 18(a) and (b) present the relationship between the water content and undrained shear strength after electrokinetic treatment and diffusion phases in the vicinities of the anodes and cathodes, respectively. The change in strength may be attributed to the processes operating in the tests, including:

(a) aging – a process of bond growth with time without introduction of external agents (Leonards and Ramiah 1959, Bjerrum and Lo 1963);
(b) electroosmotic consolidation – a process of electrically induced water flow from anode to cathode (see e.g. Casagrande 1949, Mitchell and Wan 1977, Lo and Ho 1991); and
(c) deposition of cementation bonds under ionic diffusion.

The small increase in strength in the control samples after 52 days may be attributed to the process of aging under the constant applied stress of 15 kPa. During electrokinetic treatment, all three processes would be operating but the dominant mechanism is electroosmosis as can be seen by the large decrease in water content at the anode region and little change in water content at the cathode region. Finally, after the current is switched off, the mechanism operating would be ionic diffusion with a small contribution from aging. During this period, deposition of cementation bonds predominately occurs.

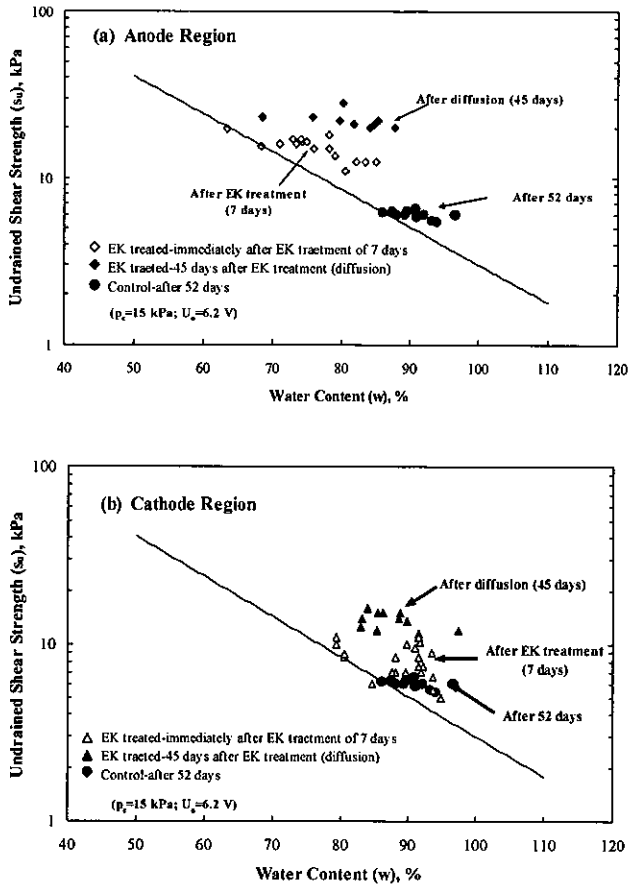

Figure 18. Undrained shear strength versus water content: (a) at anode and (b) at cathode

Figure 19 illustrates the development of strength during the entire experiment by following the strength-water content paths starting from an initial water content of 95%. At the anode region, the shear strength increased from 4.5 kPa to 16.5 kPa immediately after electrokinetic treatment along with a decrease in water content from 95% to 74%. The undrained shear strength further increased from 16.5 kPa to 21 kPa after a diffusion phase of 45 days in spite of an increase in the soil water content from 74% to 85%. At the water content of 85%, consolidation alone as indicated by the results of the control test would yield a strength value of 7 kPa. Thus, the strength contribution from bonding amounts to 67% of the total strength.

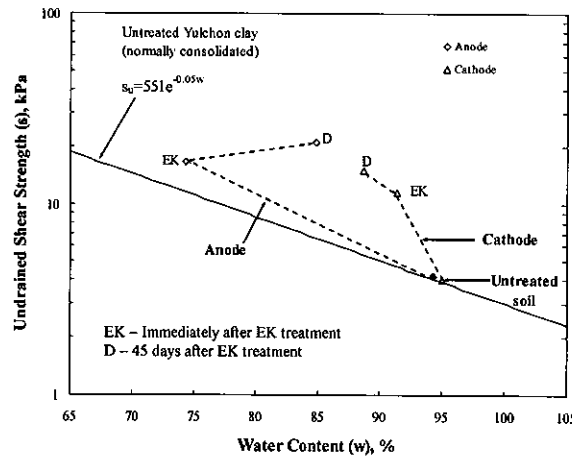

Figure 19. Development of the undrained shear strength and water content changes of the Yulchon Clay during and after EK treatment

At the cathode region, the undrained shear strength increased from 4.5 kPa to 11.5 kPa immediately after electrokinetic treatment along with a decrease in water content from 95% to 91%. The shear strength further increases from 11.5 kPa to 15 kPa after 45 days of the diffusion phase along with a slight decrease in water content from 91% to 87%. At water content of 87%, consolidation only would yield an undrained strength of 5.4 kPa. Thus, the strength from bonding would constitute 64% of the total strength.

The stress-strain curves from unconfined compression tests on treated soil are presented in Figure 20. As can be seen, the results of compression tests are consistent with the results of vane tests discussed earlier, showing that the undrained shear strength increased due to EK treatment. In addition, brittleness developed in the soil as a result of electro-cementation. It is also noted that the brittleness is more prominent at the cathode than at the anode region, which is consistent with the strength development paths in Figure 19.

Oedometer tests were performed on specimens from the anode and cathode region as well as from the control test. The results are shown in Figure 21. It may be seen that a preconsolidation pressure of approximately 40 kPa has developed in both the anode and cathode region as a result of electro-cementation. The control test gives a preconsolidation pressure of 16 kPa compared with the applied pressure of 15 kPa. It may therefore be observed that an overconsolidation ratio of about 2.5 has been induced by cementation bonding.

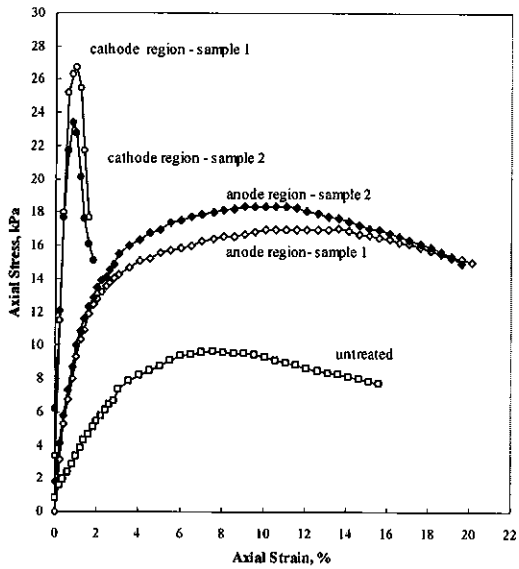

Figure 20. Results of unconfined compression tests

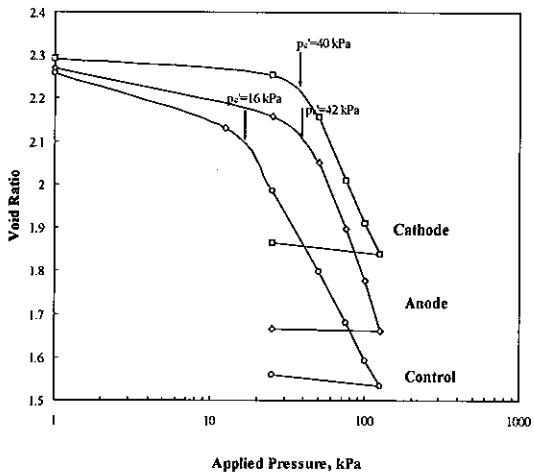

Figure 21. Results of consolidation tests on Yulchon Clay

The mechanism of this electro-cementation may be attributed to selective sorption and ionic exchange of ionic species on clay particle surfaces and precipitation of amorphous chemical compounds such as iron oxide/hydroxide and calcium carbonate which serve as cementation agents (Quigley 1980). X-ray fluorescence (XRF), specific surface and cation exchange capacity (CEC) analyses were performed on the soil samples to detect the chemical changes in the soil due to electrokinetic treatment and to identify cementing agent(s) involved. The XRF analyses provide the major element composition of the soil. The results of the analyses shown in Table 5 show that the percentage of iron oxide (Fe_2O_3) increased significantly in the soil after electrokinetic treatment while the percentages of other oxides (e.g. SiO_2, TiO_2, Al_2O_3, MnO, MgO, CaO, K_2O, Na_2O, P_2O_5, Cr_2O_3) only slightly changed. In particular, the percentage of iron oxide increased from 5.7% up to 11.8% while the percentage of other potential bonding agents of SiO_2 and Al_2O_3 showed no increase. The increase in iron oxides is also confirmed by the change in the soil colour from grey to yellowish-brown in the zone of influence of electrokinetic treatment. The source of the iron was from the steel electrodes, which corroded during the electrokinetic treatment. The released iron precipitated as oxide or hydroxide due to the extremely low solubility of iron in the normal pH range of soils. The iron oxide adsorbed on soil particle surfaces induced a cementation effect that led to the consequent development of strong aggregation of soil particles and thus an increase in the soil shear strength.

The results of specific surface and CEC analyses of the treated soil are listed in Table 6. For comparison, the corresponding values of untreated soil are also included in the table. It can be seen from the table that the values of specific surface and CEC of the electrokinetically treated soil particles were higher than those of untreated soil. This increase in specific surface area, and thus in the CEC, also indicates the presence of the higher content of iron oxides in the treated soil because it is known that iron oxides have high specific surface area amenable to act as coating on other particles (Dixon et al. 1977).

Table 5. Results of XRF analyses of Yulchon Clay

Oxides (%)	Control	EK Treated Soil
SiO_2	56.55	49.90
TiO_2	0.72	0.64
Al_2O_3	16.70	14.61
Fe_2O_3	5.74	11.78
MnO	0.09	0.13
MgO	2.41	1.82
CaO	1.23	2.50
K_2O	2.96	2.60
Na_2O	1.67	1.39
P_2O_5	0.10	0.95
Cr_2O_3	0.01	0.02
L.O.I.	11.60	13.10
Total	99.78	99.45

Table 6. Results of post-treatment chemical tests

Properties	Control	EK Treated Soil
Iron Oxide Fe_2O_3 (%)	5.7	11.8
Specific Surface (m^2/g)	23	34
CEC (meq/100g soil)	6.7	26.4
Iron Fe (Wt%)	8	36

In addition, the Energy Dispersive X-ray (EDX) analyses were performed to identify the elemental composition of the soil. The average of the percentage of iron per total weight of the untreated soil was approximately 8 Wt%, while the percentage of iron after treatment was about 36 Wt%.

The microscopic structure of the Yulchon Clay before and after EK treatment was studied using a scanning electron microscope (SEM). The SEM analyses were undertaken in order to visually identify the occurrence of cementation in the soil due to electrokinetic treatment. Figures 22(a) and (b) show the surfaces of the untreated (control) and treated soils, respectively. It is evident that some amorphous cementation compound(s) were formed and precipitated on the clay particles.

(a)

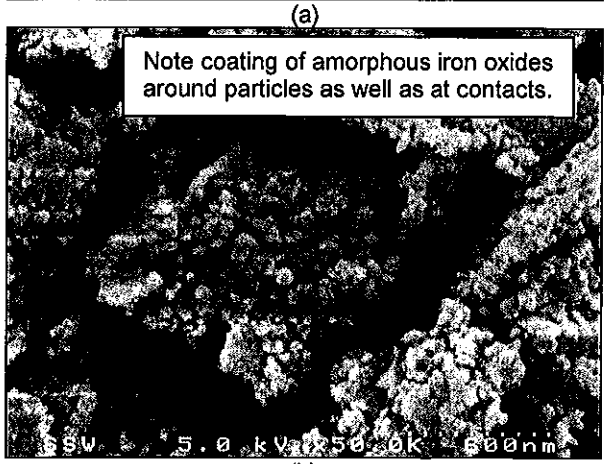

(b)

Figure 22. Electron microscopy images of Yulchon Clay: (a) Control samples; (b) EK treated samples

Finally, it is noted that the iron oxide (Fe_2O_3) has been measured in natural St. Alban and Gatineau Clay (Yong et al. 1979) with values of 5% and 6%, respectively. These values are comparable to that of Yulchon Clay used in the experiments as shown in Table 6. In addition, the authors suggested that the oxides would coat the particles. The EM image in Figure 22 lends support to this hypothesis.

From this study on electrokinetically induced cementation bonds, the following observations may be made:

(1) Iron oxides can act as an effective cementing agent in soft clays.
(2) Cementation bonds can contribute up to approximately 60% to 70% of the undrained strength of the clay with brittle behaviour.
(3) Similarly, an overconsolidation ratio of about 2.5 can be induced by electro-cementation.

5.5 Estimate of Bond Strength in Some Natural Materials

Although the existence of bonds in soft clays has been accepted by some researchers for some time (e.g. Crawford 1963, Kenney et al. 1967), direct measurement of bond strength in natural soils is difficult and their order of magnitude can only be inferred. In the case of St. Vallier Clay, the drained tensile strength is only about 3 kPa. This would represent the minimum bond strength under tensile stress induced at the contact points.

In an attempt to evaluate the bond strength under shear, three series of CIU tests were performed on St. Vallier Clay by isotropically consolidating specimens trimmed from block samples to pressures of 140, 210 and 280 kPa and then reducing the consolidation pressure to achieve OCRs up to eight (see Morin 1975). The results of one of the series are shown in Figure 23 in which the post-peak envelope from Figure 8 is also shown. It may be observed that for OCR exceeding three, the shear strengths lie close to the post-peak envelope but not on the extension of the unstructured envelope. Similar observations may be made on results from the St. Louis Clay. The results of these tests are an additional indication of the robustness of the post-peak envelope. Using this envelope as the baseline reference, the maximum bond strength under shear for St. Vallier Clay would be about 20 kPa and represents about 30% of the shear strength in the effective stress region considered. Similar results were also obtained for St. Louis Clay.

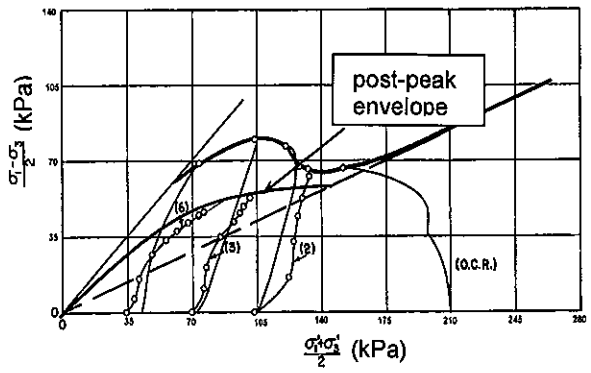

Figure 23. CIU-OC tests, i=0°, Initial σ_c'=210 kPa, St. Vallier Clay

Substantially higher bond strength may exist in stiff quick clays in the lower St. Lawrence region. The soil involved in the Toulnustouc Slide (Conlon 1966) has a liquid limit of 22, plasticity index of 4, with a high liquidity index of 3.4. The undrained shear strength is 400 kPa. A drained tension test indicated that the minimum tensile bond strength is about 17 kPa. The bond strength in shear may be interpreted to be as much as 350 kPa.

Quigley (1968) performed a mineralogical analysis on a small block sample of the clay and reported "the strong bonding exhibited by the Toulnustouc Clay is also related to aluminium and iron hydroxide precipitates in the soil. These materials probably form bonds in two ways: (1) by direct precipitation to form a cement linking the soil grains together, and (2) by growing in the mineralogical continuity at the edges of the clay crystals, thus increasing their size. The latter would result in increased Van der Waals attractive forces as crystals grow closer together and could even form cementation bonds if the crystals came into contact with one another." The reasonableness of this hypothesis has been supported by the results of the artificial cementation study in Section 5.4.

An example of very large bond strength is described in Leroueil and Vaughan (1990) for a mudstone in Japan (Ohtsuki et al. 1981). An examination of their data shows that in the normal stress range from 1500 to 3000 kPa, the friction angle ϕ' is only 8° with the shear strength of about 1800 kPa. In this stress range, the shear strength mobilized is therefore mostly bond strength.

It can be observed from these cases that while the bond strength in tension is low, the bond strength in shear of natural material may differ by three orders of magnitude and may constitute the major component of the total shearing resistance that are measured in conventional tests in some natural materials. The degree to which it can be mobilized depends on the nature of the engineering problem under consideration.

6. ANALYSIS OF THE VERNON EMBANKMENT

6.1 Brief Description of Failures

A dramatic and most instructive case history was presented by Crawford et al. (1995) who described two consecutive failures of an embankment on soft clay, in spite of the fact that two test embankments were already constructed on either side of the failures and that the test embankments were higher than the embankments that failed. The site is at Vernon, British Columbia. The subsoil conditions shown in Figure 24 consisted of approximately 4 m of interlayered sand, silt and clay, followed by a 5 m thick stiff to very stiff clay crust, then by a deep deposit of soft to firm silty clay. The undrained shear strengths measured by field vane tests were approximately 80 kPa in the stiff clay and 30 to 40 kPa in the soft to firm clay. The plasticity index was about 35 and the natural moisture contents varied from 60% to 80%. Figure 25 shows the locations of the test embankments and the embankment that failed twice. The west test embankment was constructed to approximately 11.5 m thickness. The east test embankment with wick drains was constructed to 12 m. The test fills were well instrumented. Pore pressures and settlements were measured during the construction of the test fills and the road embankment.

Construction of the road embankment started in early December 1988 and slowly filled to 7 m to 9.5 m along the alignment by June 30, 1989, when the first failure occurred on the north side encompassing a portion of the east test fill, as shown in Figures 25 and 26. The test fill had been in place since 1986, and according to results of monitoring, all excess pore pressures had dissipated (see Fig. 12 of Crawford et al. 1992). The failure was deep-seated and probably circular. It appears that the only significant warning sign was that the ratio of pore pressure increase to applied loading increase $\Delta u/\Delta p$ approached one within the failure zone. The pore pressure response to embankment load within the failure area is shown in Figure 27.

Reconstruction of the embankment was carried out by adding 5 m thick and approximately 30 m wide berms on both sides of the failure. Filling started in August 1989 and progressed at a very slow rate. On March 10, 1990, a second failure, much larger in extent and including most of the first failure, occurred between the two test fills that had been in existence since 1986 (Figures 25 and 26). The height of the fill at the time of the second failure was 11.2m, which is somewhat higher than that of the first failure. The road was eventually completed with berms and lightweight fill.

This case record, with test fills and well executed instrumentation and monitoring, led to several obvious but perplexing issues.

1. Why was the observational approach, which is generally accepted and now a time-honoured

method, not successful in preventing either the first or second failure?

2. In what way are the results of the two test fills misleading? Is the degree of natural horizontal variation of soil properties sufficient to cause the results of the test fills to be inapplicable?
3. Why did the designed provision of berms not prevent the second failure?

To investigate these issues, a series of limit equilibrium and finite element analyses were performed and the results of these analyses are discussed in the following sections.

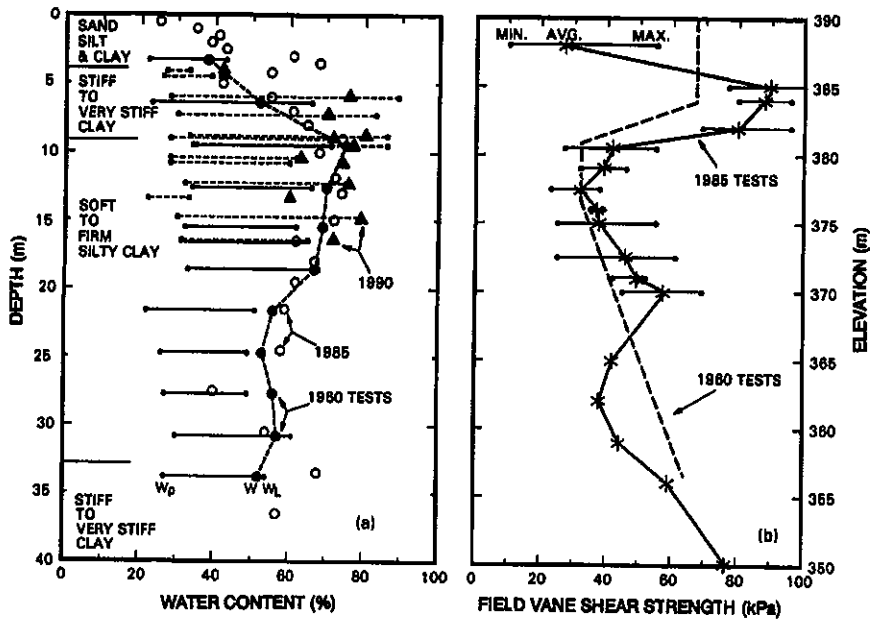

Figure 24. Profiles of water contents, Atterberg limits and shear strengths (after Crawford et al. 1995)

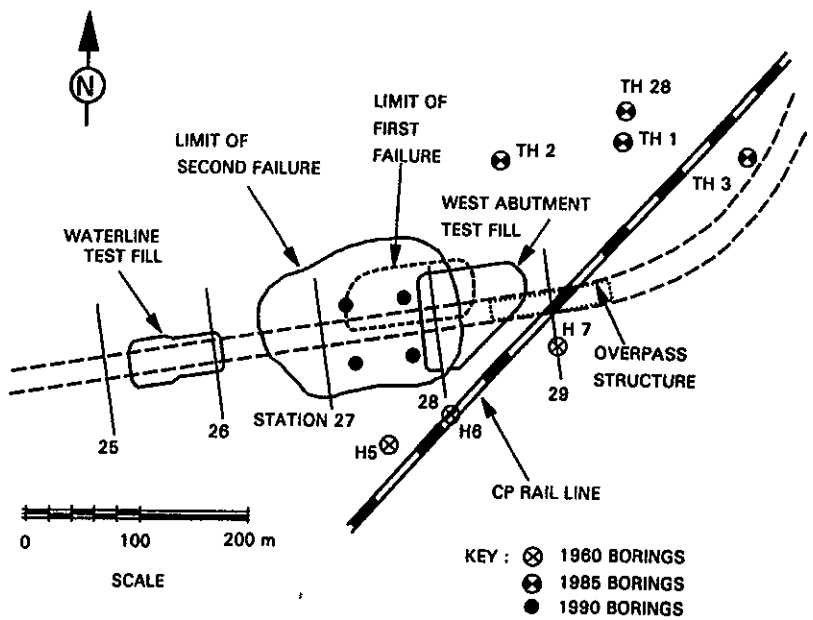

Figure 25. Site plan showing location of test fills and failure zones (after Crawford et al. 1995)

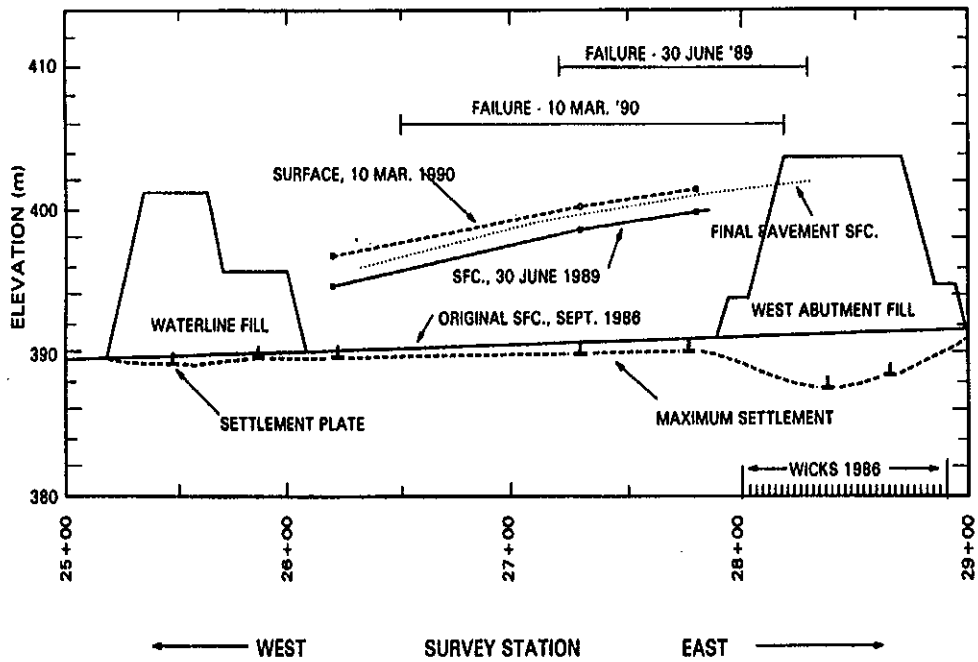

Figure 26. Longitudinal section through the embankment (after Crawford et al. 1995)

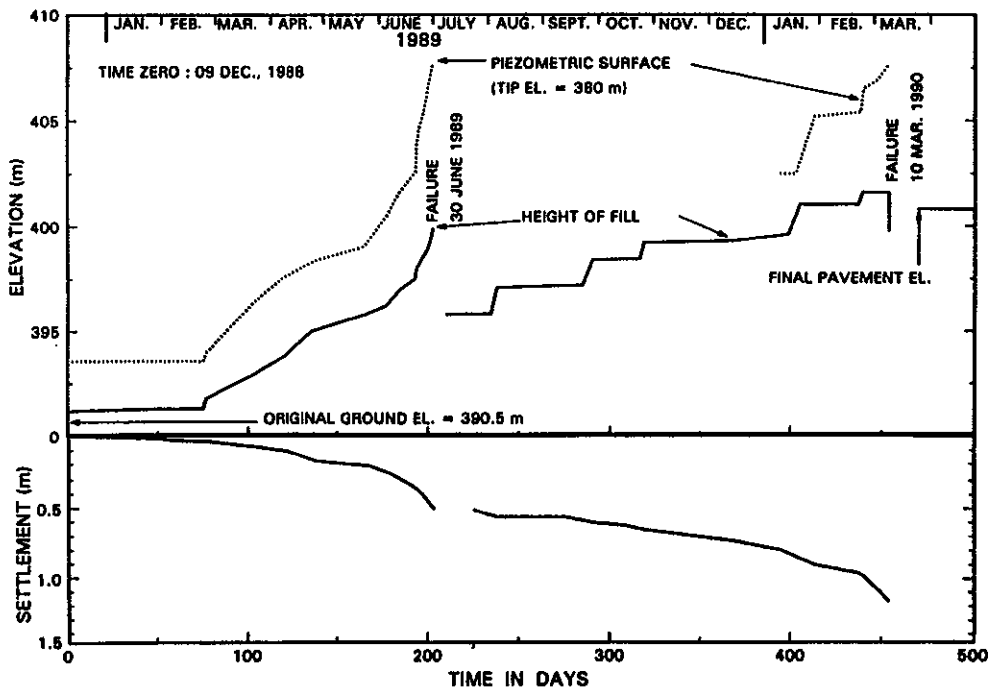

Figure 27. Height of fill, settlement, and piezometric surface at centre line of station 27+80 during construction (after Crawford et al. 1995)

6.2 Limit Equilibrium Analyses

Crawford et al. (1995) performed stability analyses for the first failure assuming a uniform undrained strength in both the crust and in the soft clay layer below the crust. The results of their study showed that a factor of safety of approximately one could be obtained for a crust strength of 50 kPa and a strength of 30 kPa in the soft clay layer below the crust.

A more detailed representation of the subsoil strength profiles will be used in this paper based on the vane strength data shown in Figure 24. In accordance with the observations on the effect of fissures on the mass strength discussed in Section 4, the strength of the crust was corrected to 40 kPa down to a depth of 6 m where the strength decreases in the transition zone to 9 m depth from which the strength increases linearly with depth. Bearing in mind that the depth of the slip surface lay within the first 15 m depth, three strength profiles are shown in Figure 28, together with the 1960 and 1985 measured vane strength. It is considered that the middle profile marked M appears to be the most representative of the vane strength data while the higher (by ~ 20%) strength profile marked H and the slightly lower (by ~ 10%) strength profile marked L are obviously within reasonable limits of interpretation of the strength data. The material parameters of the fill used were unit weight of 20.4 kN/m^3 and c'=0, ϕ'=33°, as in Crawford et al. (1995). Table 7 summarizes the material parameters used in the analysis.

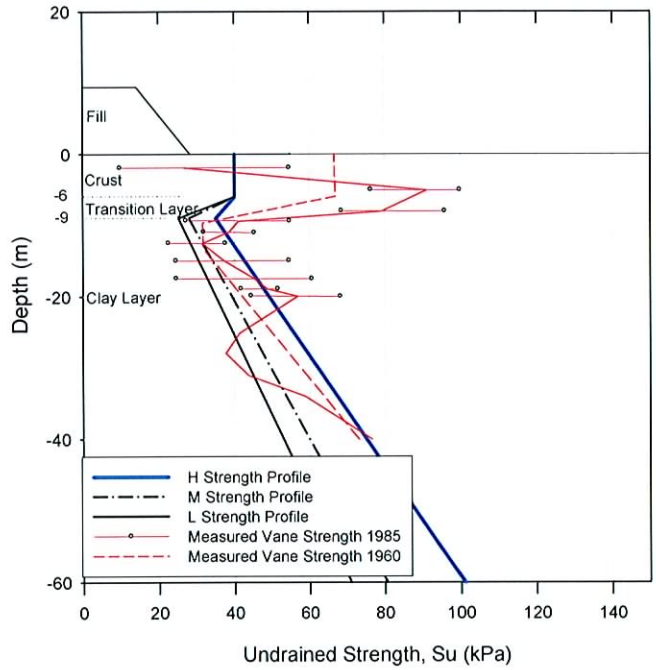

Figure 28. Distribution of vane strength with depth (adopted from Crawford et al. 1995)

Table 7. Material properties used in the limit equilibrium analysis of the Vernon Embankment

	Depth(m)	Strength Profile (kPa)			Unit Weight, γ (kN/m^3)
		H	M	L	
Crust Layer	0 -6	40	40	40	20
Transition Layer	6 - 9	40 - 35	40 - 28	40 - 24.5	17
Soft-Stiff Clay Layer	9 - 40	35 - 75	28 - 60	24.5 - 52.5	17

Table 8. Factor of safety with different strength profiles

	The First failure	The Second failure
	FS	FS
H Strength Profile	1.19	1.29
M Strength Profile	1.07	1.13
L Strength Profile	1.00	1.04

The results of stability analysis are shown in Table 8. It may be seen that, for the first failure, both the M-profile and the L-profile yield a factor of safety not far from one. As discussed earlier, both profiles are within reasonable limits of interpretation of measured vane strength data. Without correction for crust strength, the factor of safety would be 1.3. The factors of safety for the second failure are slightly higher than the corresponding ones of the first failure but are still within the limits of reliability of ϕ=0 analysis. It is recognized that part of the fill would have settled into the subsoil rendering the results somewhat difficult to interpret. Nonetheless, the results of the second failure may be considered as supplementary evidence, which is consistent with results of analysis of the first failure.

From the discussions in the preceding paragraphs, it is apparent that the instability condition of the Vernon Embankment is similar to other embankments in soft to firm sensitive clays. While limit equilibrium analysis might have (from hindsight) predicted the instability of the two failures, conventional stability analysis alone would not have addressed the questions in Section 6.1.

6.3 Finite Element Analysis of Vernon Embankment

It has been recognized that the development of an overstressed zone (plastic region) in soft clay controls the development of high pore pressures and thus the stability of embankments with low factors of safety (Lo 1973; Law 1975). In order to explore the behaviour of the Vernon Embankment in more detail, finite element analyses were performed.

6.3.1 Method of Analysis

The first series of analyses carried out was the elastoplastic total stress analysis under plane strain condition using the program AFENA (Carter and Balaam 1995) for the two successive failures. The parameters used are the same as those in limit equilibrium analysis (Table 7). Additional parameters required are the coefficient of earth pressure at rest, K_o, which is taken to be 1.04 in the crust and 0.84 in the soft clay. The undrained elastic modulus, E_u, was evaluated assuming an E_u/S_u ratio of 500 and S_u from the M-profile in Figure 28. The fill strength used was c'=10 kPa and ϕ'=33°.

The construction of the embankment was simulated by activating the elements of fill material layer by layer, nine layers for the first failure and eleven layers for the second layer as shown in Figure 29. The mesh used is shown in Figure 30.

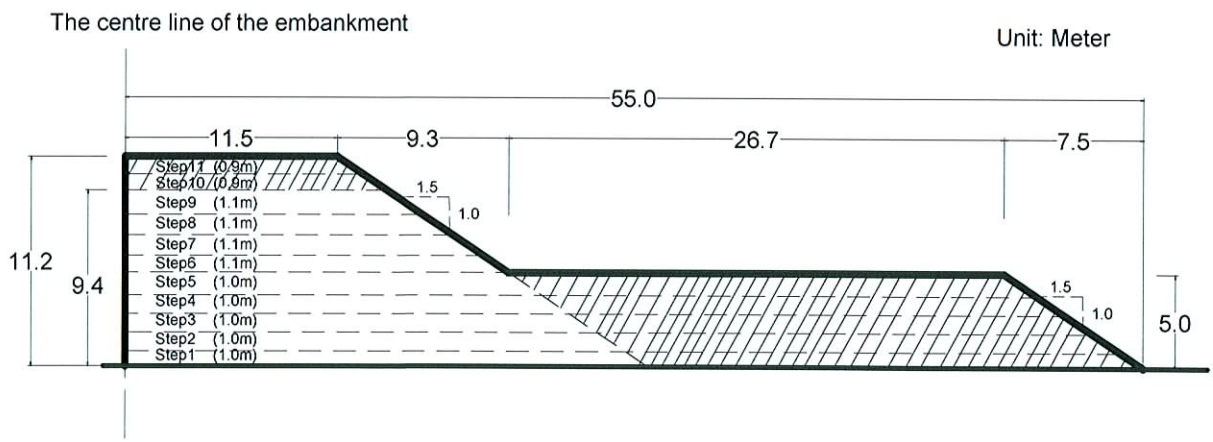

Figure 29. The numerical construction scheme (The shaded area represents the construction after the first failure)

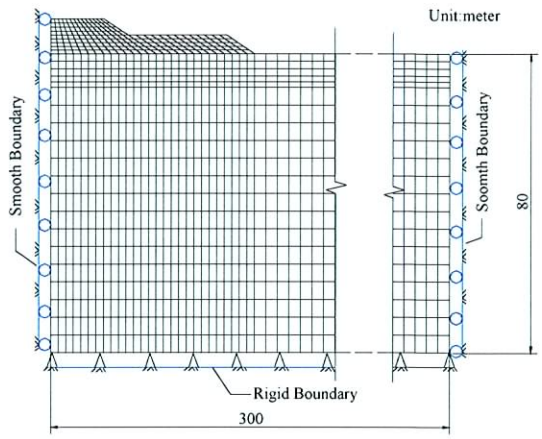

Figure 30. FEM mesh and boundary conditions

6.3.2 Results of Analysis

The incremental simulation of the construction of the embankment portrays the development of the plastic zone and velocity field. As the embankment height approaches the collapse load, the plastic region extends to the ground surface outside the embankment and a kinematic mechanism has developed as shown in the velocity field, both of which indicate a failure state is imminent or has been reached. Figure 31 illustrates the extent of the plastic zone and velocity field at an embankment height of 8.3 m (prior to failure) and 9.4 m (at failure), respectively. The distinct changes in plastic zone and velocity field when the fill height reached 9.4 m can be observed.

The propagation of the plastic zone with an increase in embankment height is shown in Figure 32 together with the velocity field boundary. The measured lateral deflection close to the toe at Station 27+80 (Figure 11, Crawford et al. 1995) is also shown. From this figure, the following observations may be made:

(a) The plastic zone starts to form in the soft clay below the crust and engulfs the location of the piezometer at 10 m depth when the embankment height reaches 4 m at Stn. 27+80. Subsequent to the yielding of the soil at this moment, an increase in rate of pore pressure rise may be expected. Figure 33 shows the measured pore pressure with an increase in embankment height. It can be seen that the yielding of the clay is well indicated by the results of pore pressure measurements.

(b) The depth and the overall location of the velocity field boundary are in general agreement with the slip surface deduced by Crawford et al. (1995); and

(c) The horizon of maximum deflection at failure agrees well with the location indicated by the results of inclinometer measurements.

(a) Plastic Zone (H=8.3 m)

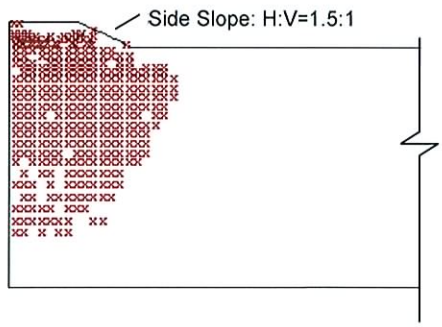

(b) Velocity Field (H=8.3 m)

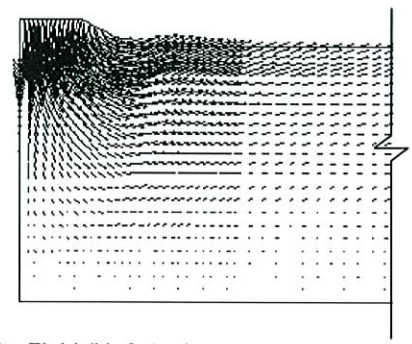

(c) Plastic Zone (H=9.4 m)

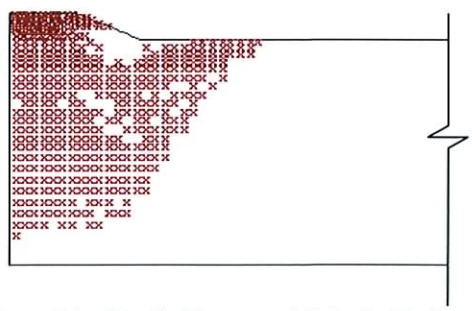

(d) Velocity Field (H=9.4 m)

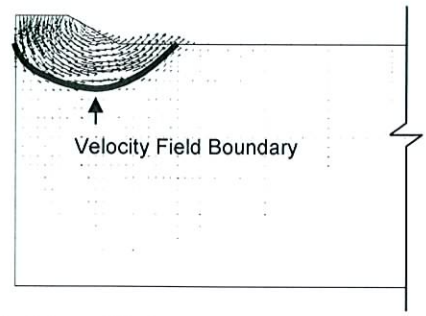

Figure 31. Plastic Zones and Velocity Fields at embankment heights of H=8.3 m and H=9.4 m

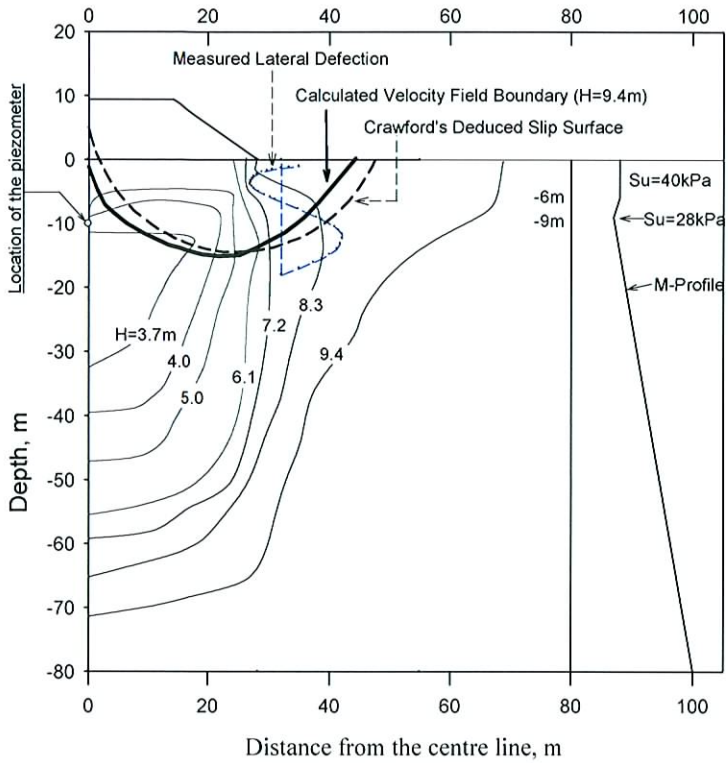

Figure 32. Development of plastic zone in the foundation at increasing embankment height

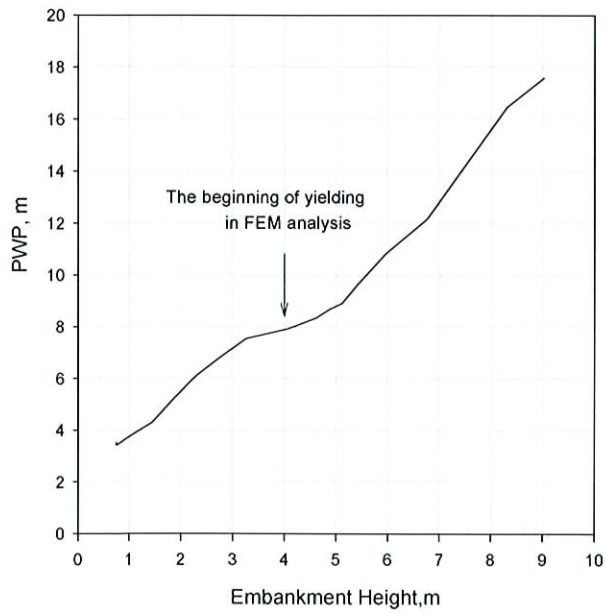

Figure 33. Measured pore water pressure on -10m depth at centre line of station 27+80

The effect of strength profiles on the prediction of the critical height of the embankment is shown in Figure 34. It can be seen that the H-profile over predicts, the L-profile under predicts slightly and the M-profile yields good agreement with the observed critical height of 9.4 m for the first failure. The computed settlement with embankment height relationships are compared with the measured settlements in Figure 35. Bearing in mind there would be some effect of partial consolidation, it can be seen that there is overall consistency between the results of the M-profile and the observed settlements.

From the discussion in the preceding sections, it is apparent that there is overall general agreement between the results of analysis and the observed field behaviour including critical height, pore pressure, lateral deflection, settlement and position of the slip surface.

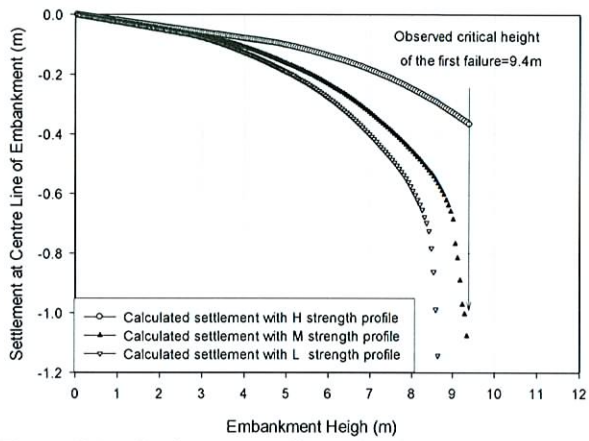

Figure 34. Settlement of embankment centre vs embankment height with different strength profiles at station 27+80 (the first failure)

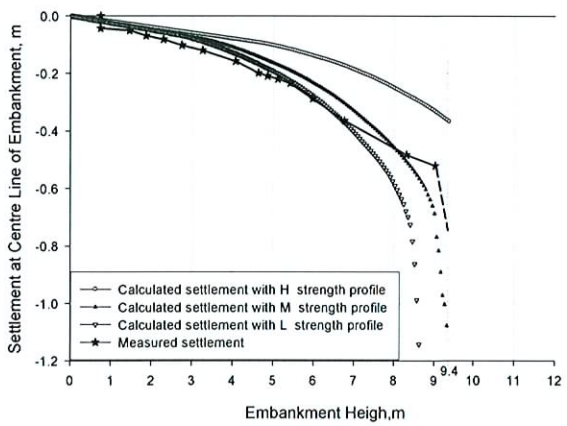

Figure 35. Measured and calculated settlements of the embankment centre station 27+80 (the first failure)

6.3.3 Results of Analysis of Second Failure

Similar analyses were carried out for the second failure using the same parameters as for the first failure. The results of computed embankment height versus settlement relationships for the three strength profiles are shown in Figure 36. The results for the L-profile yield agreement with the observed critical height of 11.2 m. One interpretation would be that this might indicate an overall loss of strength of about 10% after the first failure due to disturbance. This interpretation would be consistent with the factors of safety computed in Table 8.

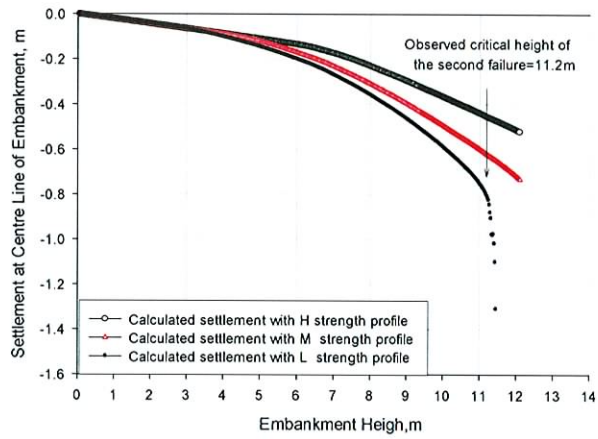

Figure 36. Vertical displacement of embankment centre vs embankment height with different strength profiles at station 27+80 (the second failure)

6.3.4 Analysis of Waterline Test Fill

Two test fills were successfully constructed on the west (Waterline Test Fill) and east (West Abutment Test Fill) of the two failures as shown in Figure 25. Because the performance of the West Abutment Test Fill was affected by the installation of prefabricated vertical (wick) drains, only the Waterline Test Fill will be analyzed so as to investigate the difference in behaviour between the failed embankment and the stable condition of the Waterline Test Fill.

An examination of the geometries of the Waterline Test Fill shows that the problem is closer to three-dimensional than a plane strain condition. Therefore, any plane strain analysis (including limit equilibrium analysis) based on plane strain condition may be misleading. Although a 3-D elastoplastic analysis would be preferable, a simpler axi-symmetric analysis was performed so as to obtain some insight, as a first approximation, into the impact of geometry on the vast difference in behaviour of the embankments. The rectangular geometry of the Waterline Test Fill was idealized to a circular load with its diameter equal to the average dimension of the two sides. Figure 37 shows the progress of the plastic zone from 9 m to 11.2 m to which the test fill was successfully completed. It is evident that at 11.2 m, the condition is that of a contained plastic zone and the test fill is stable. (A conventional limit equilibrium analysis with the M-

profile would have shown that the factor of safety would be well below unity. In contrast, a back analysis assuming a factor of safety of one would have indicated high strength. Both results would be misleading.)

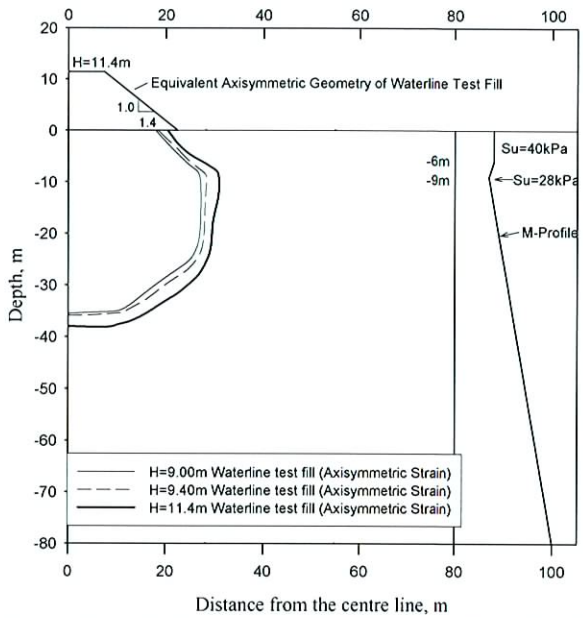

Figure 37. Development of plastic zone under Waterline test fill (Axi-symmetric strain assumption)

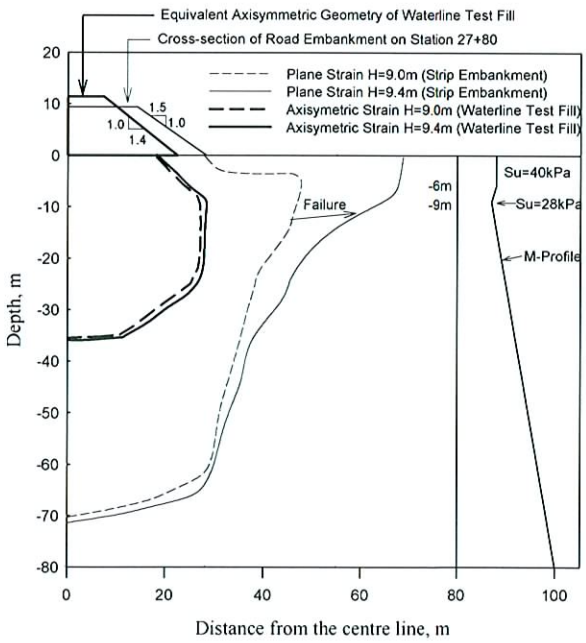

Figure 38. Development of plastic zones under Waterline test fill and strip embankment at station 27+80

The plastic zones at H=9.0 m and H=9.4 m for a strip and circular embankment are shown in Figure 38. The large difference in extent of the plastic zones due to different geometries of loading is evident. In addition, the propagation from 9.0 to 9.4 m is quite small for the circular load. In contrast, the increment 0.4 m of loading for the strip embankment results in continuous plastic zone to the ground surface leading to collapse.

It is therefore suggested that observations at the Waterline Test Fill may not be directly applicable to the road embankment due to the difference in development of the plastic zone under different loading configurations.

In a subsequent section, case records of well defined loading geometries will be analyzed to verify the findings discussed for the Vernon case records.

7. EFFECT OF EMBANKMENT GEOMETRY ON BEHAVIOUR OF FOUNDATION CLAY

In order to verify the effect of geometry of the overlying embankment on the soft clay in the case of the Vernon embankment and the test fill, a case record of well defined geometries of surficial loading on a soft clay deposit is examined.

The impact of embankment geometry on the behaviour of the foundation soil has been studied by Lo (1973) and Law (1975). The case of the Skå-Edeby Test Field constructed and monitored over a period of more than ten years is examined.

7.1 Skå-Edeby Test Field

In 1957, the Swedish Geotechnical Institute constructed a series of test fills at the Skå-Edeby test field situated 25 km west of Stockholm Sweden. Figure 39 shows a plan of the test site showing the locations and dimensions of each test fill. Originally, four circular fills were constructed at Skå-Edeby of which three fills, Areas I, II and III, were provided with sand drains at different spacing to accelerate primary consolidation of the underlying foundation clay; a fourth test fill, Area IV, was built without sand drains. In 1961, four years after construction of the original circular fills, a 40 m long test embankment was constructed at Skå-Edeby by unloading Area III (see Figure 39). The test embankment had a crest width of 4 m and it was built without sand drains permitting comparison of its performance with that of Area IV. Holtz and Broms (1972) provide a detailed account of the performance and assessment of the circular test fills whereas the plane strain embankment is described by Holtz and Lindskog (1972). For both the embankment and Area IV, the height was 1.5 m with an applied surface loading of 27 kPa, giving a factor of safety of 1.5.

Based on the case record, the foundation conditions at Skå-Edeby comprise an upper deposit of post-glacial clay underlain by a lower deposit of normally consolidated glacial clay. Figures 40 and 41 summarize the natural moisture content, Atterberg limits and the field vane strength profile (SGI vane) for the soils encountered below the embankment and test Area IV. For both the

test fills, the field vane strength profiles were measured prior to construction, in 1957 for Area IV and in 1961 for the embankment, and again in 1971.

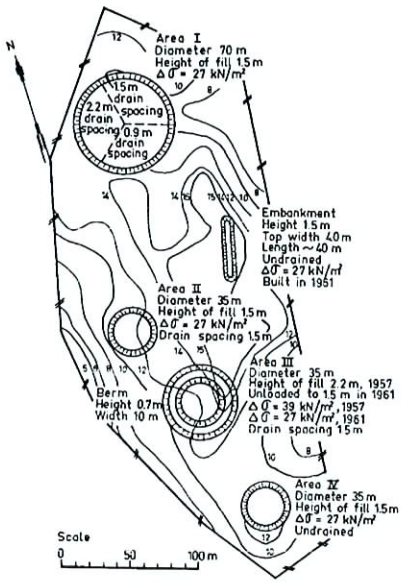

Figure 39 Plan of the Skå-Edeby test field (after Holtz and Broms 1972)

Referring to Figure 40, before construction, the undrained strength of the clay below the test embankment was only 12 kPa near the ground surface decreasing to about 8 kPa at a depth of 3.8 m. Below 3.8 m, the undrained strength increased from 8 kPa to 14 kPa at 10 m and to 25 kPa at a depth of 14 m. Below test Area IV (Figure 41), the undrained strength of the clay was found to decrease from 25 kPa near the ground surface to about 8 kPa at a depth of 3 m. The strength then increased from 8 kPa at 3 m to 14 kPa at 8 m and finally 25 kPa at a depth of 12 m. Thus, the initial strength profiles of both areas are very similar.

However, the changes in strength with time below the two embankments are very different. Based on the case records (see Figures 40 and 41), the field vane strength below Area IV increased by about 5 kPa after 14 years of sustained loading. However, for the plane strain embankment, there is virtually no increase in the undrained strength of the foundation after 10 years of loading even though the depth of the deposit and duration of loading are comparable. Consistently, there is also little reduction in water content in the case of the embankment while there is a more discernable reduction of water content in Area IV. To investigate the possible cause of this behaviour, the test embankment and Area IV fill were analyzed using the finite element method.

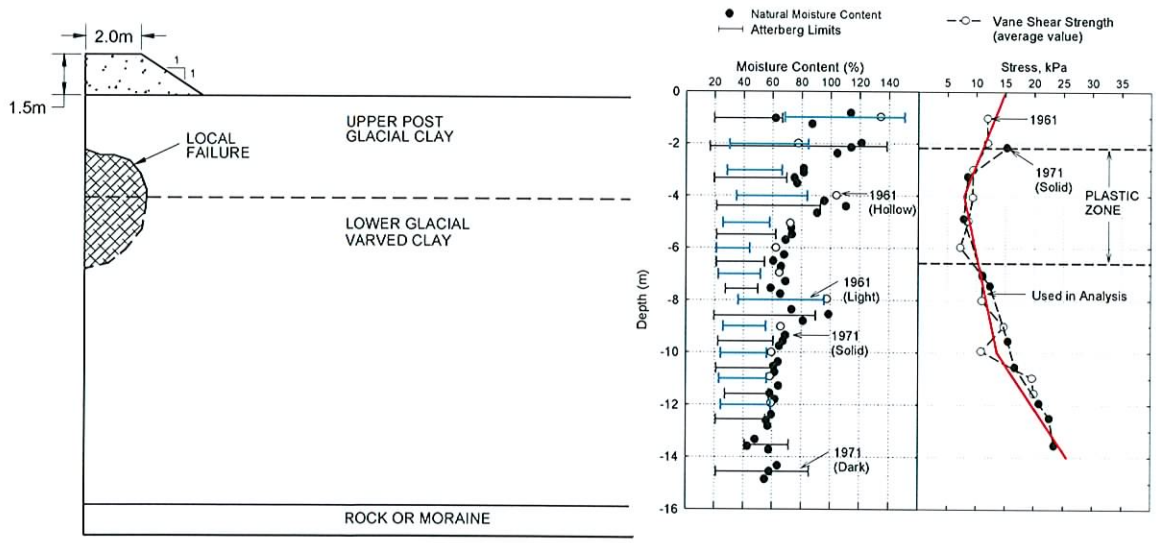

Figure 40. Skå-Edeby Test Field – Zones of local failure and subsurface profile from the plane strain test embankment (soil properties from Holtz and Lindskog 1972).

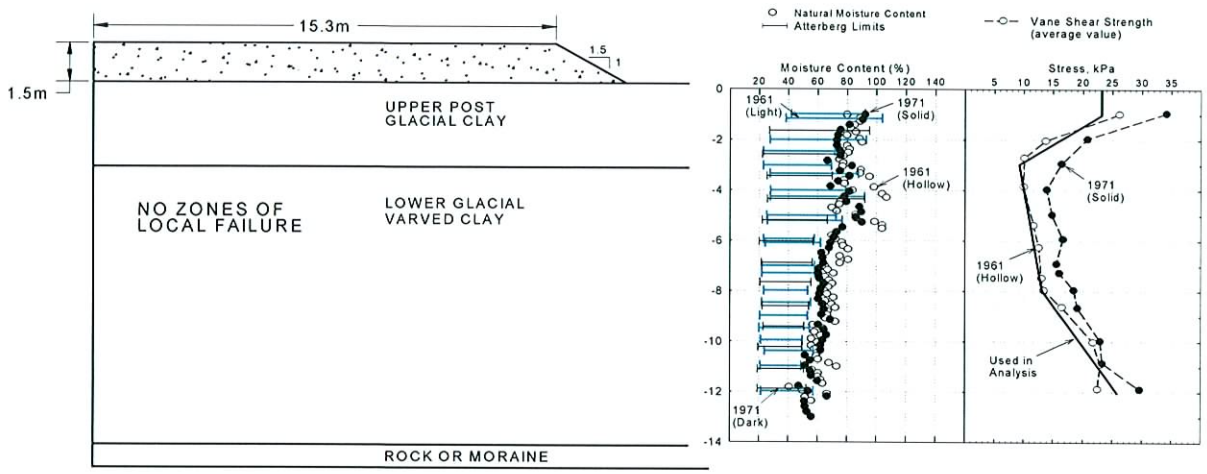

Figure 41. Skå-Edeby Test Field – Zones of local failure and subsurface profile for the circular test fill area IV (soil properties from Holtz and Broms 1972)

The undrained shear strength profile for the embankment and Area IV adopted for the analyses are shown in Figures 40 and 41, respectively. For each case, the foundation and embankment soils were modeled as linear elastic-perfectly-plastic materials with an undrained strength governed by Mohr-Coulomb's failure criteria, a Poisson's ratio of 0.49 (e.g. constant volume deformation) and an E_u/S_u ratio of 500. The finite element analysis was performed using the program PLAXIS taking care to ensure enough elements and load increments were used to obtain reliable solutions. For the test embankment, plane strain conditions were assumed since the length of the embankment was approximately ten times the crest width. Axi-symmetric conditions were assumed for the Area IV fill which was circular. The construction of each embankment was simulated in six lifts and the results of the analyses are summarized in Figures 40 and 41 which show the calculated zones of failure in the foundation after construction. It is noted that the results of the present analysis are very similar to the results obtained by Law (1975).

It can be seen by comparing Figures 40 and 41 that there is a significant extent of plastic zone in the foundation of the Skå-Edeby test embankment whereas there is no plasticity in the foundation of the Area IV fill. This illustrates the importance of the loading geometry on embankment performance as in the Vernon case described previously.

It is concluded from this study that the main difference in behaviour of Area IV compared with that of the test embankment is due primarily to the loading geometry and its consequent effect on stresses and zones of failure in the embankment foundation (see also Law 1975). Given the sensitivity of the Skå-Edeby Clay which was generally in the range of 7 to 20, it is most probable that the effect of the microstructure is significant. Therefore, the absence of strength gain below the embankment fill after ten years of sustained loading may be attributed to the process that the clay was 'destructured' within the zone of local failure. In contrast, no plastic zone exists below the circular fill Area and the behaviour of the clay follows the classical concept of strength increase with time of sustained loading.

7.2 Observations From the Study of the Vernon and Skå-Edeby Embankments

From the results of analyses of the two embankments, it is evident that the behaviour of embankments founded on soft clay depends not only on the properties of the foundation soil but also on the configuration of the applied loading. With respect to the issues raised in Section 6.1 regarding the failures of the Vernon Embankment, it may be observed that:

(a) Results of observations on test fills should be based on geometrically similar surface loading and accompanied by appropriate analyses before the results thus verified are applied to the full scale structure.
(b) Examination of the available information in Crawford et al. (1995) shown in Figures 24 and 25 indicates there is no definite trend of variation of vane strength or water content between the 1960, 1985 and 1990 investigations for the soft to firm clay layer. While there is some variation in the stiff to very stiff crust, the reduction of vane strength in the crust to account for fissures in the analyses rendered the effect of variation on the results of analyses negligible.
(c) Design for remedial measures of embankments at locations of previous slides should be based on some degree of loss of strength. A slow rate of construction does not necessarily ensure stability.

(d) For embankments (plane strain) loaded close to failure, the rate of propagation of plastic zone at fill heights approaching failure is very rapid (see Figure 38 for plastic zones at fill heights 9.0 to 9.4 m). At this meta-stable state, as the critical height is approached, it is difficult to arrest an imminent instability.

8. LONG TERM FAILURE UNDER LOADING CONDITIONS

In clays with pronounced macrostructures mainly constituted by fissures, first time slides of excavated slopes under long term conditions are well documented. For example, in cuttings in Brown London Clay, Skempton (1977) documented twelve cases with time to failure varying from immediately after excavation (Bradwell shown in Table 3) to 65 years after construction. The slopes varied in height from 5 m to 17 m and inclinations from 0.5:1 (Bradwell) to 3.75:1. However, long term failures of embankments on clay foundations are relatively infrequent. Perhaps the best known examples are the Seven Sisters dykes in Manitoba on the banks of the Red River. Large movements of these dykes, of heights between 7 to 8 m and downstream slopes of 2:1 to 2.5:1 founded on Lake Agassiz Clay had been occurring for long periods of time in the order of tens of years after construction (Peterson et al. 1960; Kuluk 1974; Graham 2003 and Man et al. 2003).

It is therefore of interest to examine the long term instability of a section of the Nanticoke dyke which failed 32 years after construction because the soil properties were comprehensively investigated in the original design, the post-construction change in the dyke geometry and pore pressure condition were reasonably known as well as the geometries of the failed and stable sections were clearly defined.

8.1 Description of the case

The Nanticoke Ash Lagoon dyke was built in Nanticoke, Ontario, between 1969 and 1970 on a deposit of stiff fissured clay. The dyke was constructed to provide containment for the storage of bottom ash and fly ash produced by the Nanticoke Thermal Generating Station. Figure 42 shows an air photograph of the ash storage area.

The Nanticoke Ash Lagoon dyke is an earthfill embankment comprising predominantly clay fill, a thin downstream granular shell comprising crushed rock and a thin zone of rockfill slope protection on the upstream slope (see Fig 44). The embankment crest width is 4m, the dyke height varies from 6m to locally 17m and the dyke has a total length of about 2130m. Initially, the Nanticoke dyke was designed and built with 2:1 upstream and downstream slopes. The dyke foundation comprises a deposit of overconsolidated (OCR ≥ 6) stiff fissured clay overlying basal till and limestone bedrock. The clay deposit is on average about 8m thick. Figure 43 shows the as-built dyke geometry and the results of limit equilibrium analysis to assess the design factor of safety, which was 1.26 for the dyke section considered below.

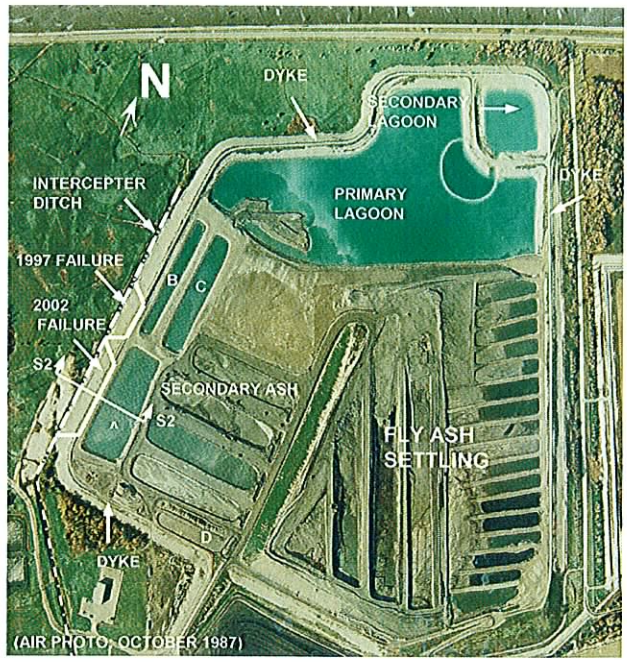

LAYOUT:
A - Secondary Ash Settling Pond 1 (normal water level el. 193.3m)
B - Secondary Ash Settling Pond 2 (normal water level el. 192.2m)
C - Secondary Ash Settling Pond 3 (normal water level el. 192.2m)
D - Bottom Ash Settling Pond (max. water level el. 195.4m)

Figure 42. Layout of the Nanticoke Ash Lagoon and Dyke

Since construction of the Nanticoke dyke, there have been three significant modifications made to the as-built dyke geometry and its operating conditions. These changes, not known at the time of the original design, are summarized in Figure 44. First, in 1971 a 3m deep interceptor ditch was added 6m downstream of the original embankment but only adjacent to the Ash Settling Ponds (see Figures 42 and 44). The ditch was built to divert runoff from fields to the west of the storage area. Then, in 1977, the downstream slope of the dyke was flattened from 2:1 to 2.75:1 using crushed rock. This modification or repair was required at all locations of the perimeter dyke due to wide spread shallow slumping of the downstream slope between 1970 and 1977. Finally, the third modification involved raising the upstream pond level from el. 189m to 193.3m in 1984 (see Section S2-S2 near Secondary Ash Settling Pond 1 in Fig 42).

After the final modifications, the Nanticoke Ash Lagoon Dyke performed satisfactorily from 1984 to 1997. However, in November 1997, a 100m long section of the dyke slumped adjacent to Secondary Ash Settling Pond 2. The location of the failure is shown on Figure 42. The dyke was subsequently repaired in 1997 by locally flattening the downstream slope to 3:1 and lowering the crest from el. 197 m to 194 m. Although the incident was

not well documented, based on the nature of the repairs it is inferred that this might be the first incident of deep-seated moment of the dyke.

In 2002, a 150 m long section of the embankment slumped adjacent to Secondary Ash Settling Pond 1 (see Fig 42). This slump was relatively well documented with photographs and some displacement monitoring. The approximately shape of the failure surface is shown on Figure 44. The time-dependent or viscous nature of the 2002 failure is of particular interest. In January 2002, the first signs of distress appeared when a 50mm wide crack was discovered on the crest of the dyke adjacent to Secondary Ash Settling Pond 1. Between January 2002 and April 2002, vertical deformations of the crest increased from initially 50 mm to nearly 1m. Horizontal deformations at the toe of the embankment increased similarly over the same period. From the observed deformations, the 2002 failure was deep seated and of a circular nature. The rate of movement during the failure, however, was relatively slow compared with documented failures in sensitive clays (for example see the Vernon case). It is interesting that the time to failure was approximately 32 years post construction making this a relatively unique case. In the following sections, the engineering properties of Nanticoke clay are discussed and the Ash Lagoon Dyke is analyzed using limit equilibrium analysis and finite element analysis to investigate the factors leading up to the 2002 failure.

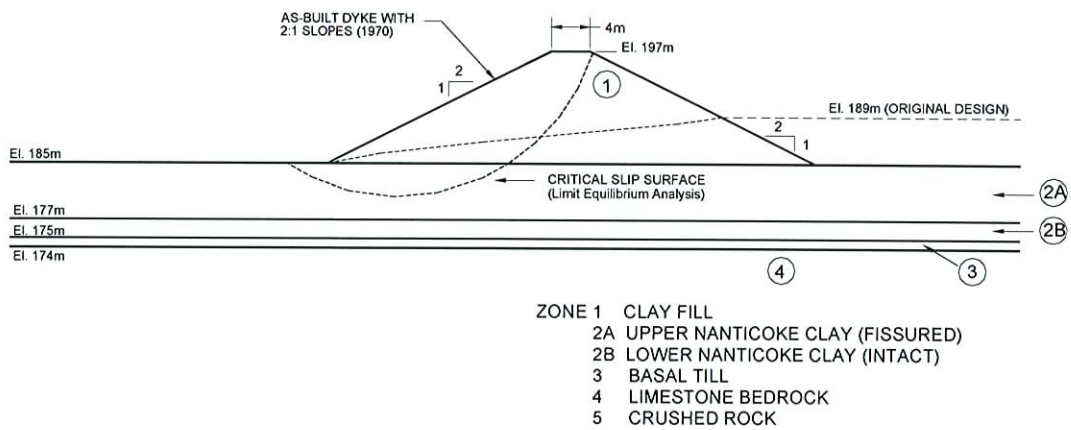

Figure 43. Original as-built geometry of the Nanticoke Ash Lagoon dyke – Section S2-S2

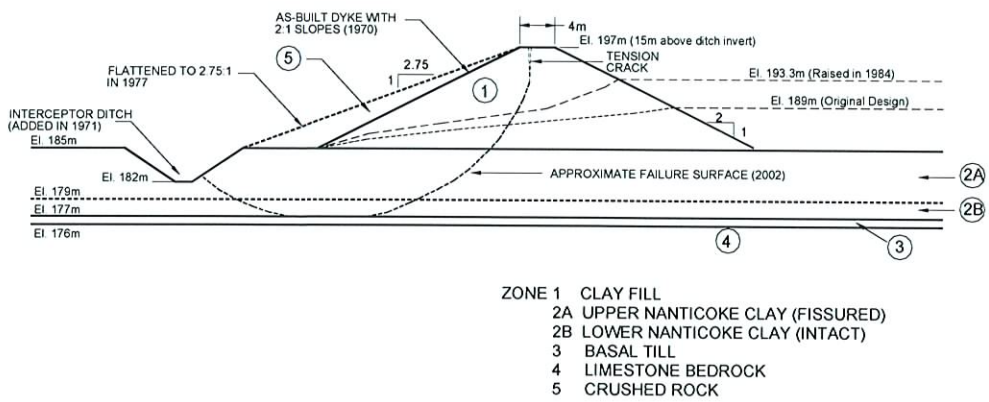

Figure 44. Summary of modifications made to the Nanticoke Ash Lagoon dyke geometry and operation after construction

8.2 Properties of the Nanticoke Foundation and Fill

The subsurface conditions at the Nanticoke site are summarized in Figure 45. The foundation of the Nanticoke dyke at Section S2-S2 comprises 8m of stiff fissured clay underlain by a very stiff to hard basal till and then limestone bedrock. In general, the stiff fissured Nanticoke clay can be divided into two basic zones. The upper zone, Zone 2A, is heavily fissured whereas the lower zone, Zone 2B, is less fissured. The impact of the relative frequency of the fissures can be seen in the variability of such parameters as the *in situ* Hydraulic Conductivity and the Standard Penetration Test N-Values (see Fig 45). The basal till and limestone encountered below the clay, although well characterized, are of lesser importance in assessing the failure.

The strength and deformation behaviour of stiff fissured clay were comprehensively investigated by Lo et al. (1969) and Lo et al. (1971). It has been shown in Figure 12 that for fissured clay there is a significant reduction of undrained strength from that of the intact material to that of the material mass as the specimen size and consequent size of the failure plane increases. Similarly, as shown in Figure 46, sample size also has an impact on the effective strength parameters of Nanticoke clay. Figure 46 shows the Mohr Coulomb envelop for Nanticoke clay as determined from drained triaxial compression tests (peak strength) and multiple pass direct shear tests (residual strength). For 18mm diameter specimens, the effective peak strength parameters of Nanticoke clay are c'=22 kPa and $\phi'=32^{\circ}$ neglecting curvature of the failure envelop at very low normal stresses: These are considered to be the peak strength parameters of the intact material. As the sample size is increased, the Mohr-Coulomb strength parameters reduce to c'=13 kPa and $\phi'=18^{\circ}$ for 100mm diameter samples, which is slightly above the residual strength of Nanticoke clay as measured using multiple pass direct shear tests (e.g. c'=13 kPa and $\phi'=15^{\circ}$). The impact of macrostructures or fissures on the engineering behaviour of Nanticoke clay is evident in Figure 46 and for stability analysis the mass strength of the material should be used: in this case $c'_m=13$ kPa and $\phi'_m=18^{\circ}$.

Lastly, in order to assess the failure of the Nanticoke dyke in 2002, the strength parameters of the dyke fill were also obtained from multiple pass direct shear tests. Both peak and residual strength parameters were obtained for the dyke material and they are summarized in Table 9. The dyke fill comprised Nanticoke clay borrowed from within the perimeter of the ash storage area and compacted at the optimum moisture content (about 26%). The residual strength of the fill and the undisturbed foundation material are identical, as would be expected.

Table 9. Material parameters used to analyze the Nanticoke dyke

Soil Layer	Hydraulic Conductivity used in the Analysis (cm/s)	Unit Weight (kN/m^3)	Cohesion Intercept (kPa)	Effective Friction Angle (degrees)	Elastic Parameters (E in kPa and ν)
Dyke Fill (compacted Nanticoke clay)	kv= kh = 5×10^{-8}	19	14†	24†	25,000 0.4
Upper Nanticoke clay (Zone 2a)	kv= kh = 5×10^{-8}	19.5	13‡	18‡	30,000 0.4
Lower Nanticoke clay (Zone 2b)	kv = kh = 1×10^{-8}	19.5	13‡	18‡	30,000 0.4
Basal Till	kv= kh = 5×10^{-7}	NA	NA	NA	NA
Bedrock	kv= kh = 5×10^{-5}	NA	NA	NA	NA

NA – Not modeled because a rigid boundary was assumed at the bottom of the Nanticoke clay deposit.
† Peak strength parameters
‡ Mass strength parameters

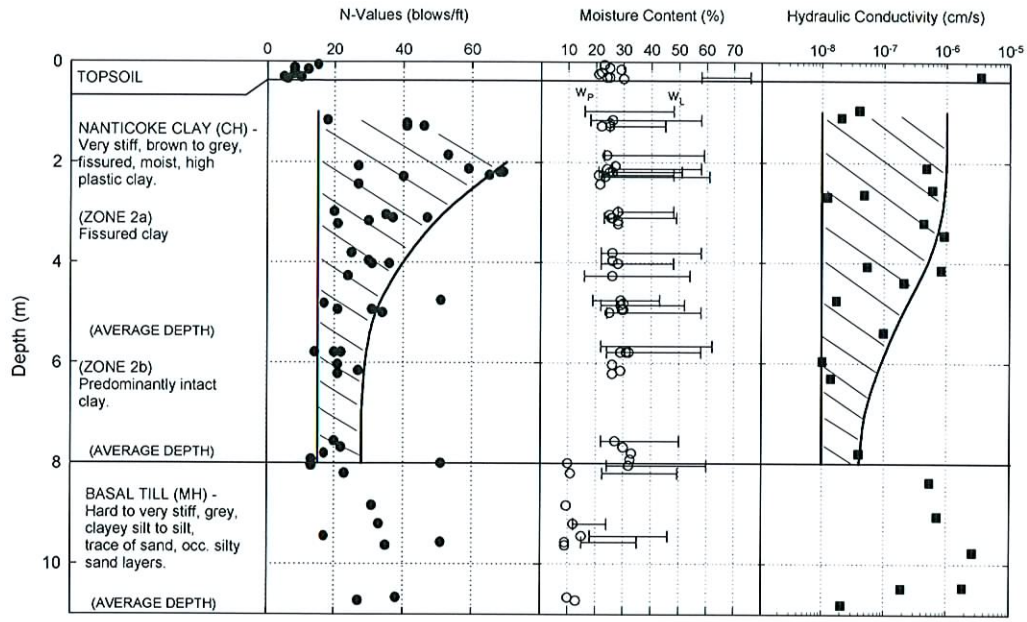

Figure 45. Subsurface conditions at the Nanticoke site.

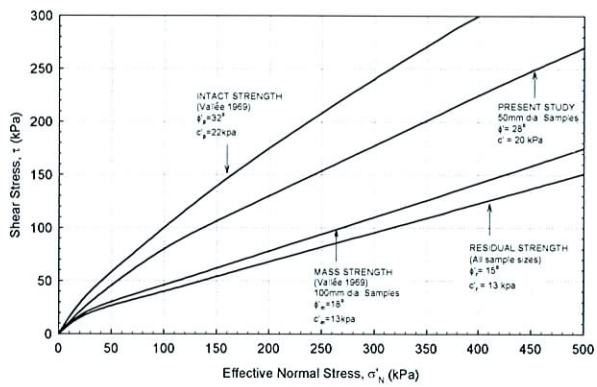

Figure 46. The effect of sample size on the effective strength envelope of Nanticoke clay (from Vallée 1969, Lo et al. 1969, and Liang 2006).

8.3 Analysis of the 2002 Nanticoke Failure

To gain insight into the stress changes in the Nanticoke case, the 2002 failure was assessed using finite element analysis. The procedure of analysis followed the stress history generated by construction and operation of the facility, so as to determine the states of effective stress and groundwater conditions at a particular stage. The material parameters used in the analysis are shown in Table 9. The initial stresses in the overconsolidated Nanticoke foundation clay were calculated assuming K_o'=1.5 with the initial groundwater table at a depth of 5.4m. In the analysis, peak strength parameters were used for the fill and mass strength parameters for the foundation.

The solution scheme involved the repeated usage of finite element seepage analysis and elasto-plastic analysis to establish the appropriate groundwater conditions and states of stress. At each stage, the results of seepage analysis were checked against field observations of pore pressures which were monitored from 1988 to 2004. The results of the analysis are shown in Figures 47a to 47d. Details of the solution can be found in Liang (2006).

Limit equilibrium calculations were also performed using the program Slope/W (Geoslope 2004) to complement the finite element analysis. The soil strength and material parameters used in the limit equilibrium analysis were identical to those used in the finite element calculations (see Table 9). For each of the operating conditions considered, the piezometric head in the dyke and its foundation was calculated by finite element seepage analysis and imported into the limit equilibrium analysis.

8.4 Discussion of Results

The impact of the significant changes in geometry and groundwater conditions since construction on the stability of the dyke have been evaluated and are discussed below. Figure 47a shows the calculated zones of plasticity or local failure in the Nanticoke case after filling the head pond to el. 189m and before excavating the downstream interceptor ditch in 1971. For the condition of the original design, the factor of safety determined from limit equilibrium analysis is 1.26 and there are small zones of local failure in the foundation near the toe of the dyke and in the centre of the fill.

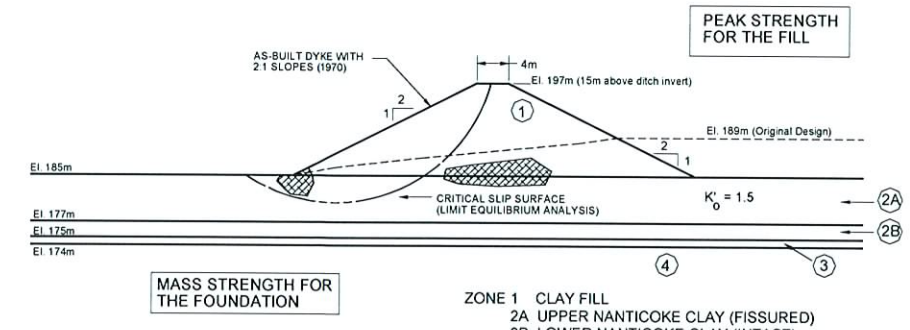

(a) Original design (FS=1.26)

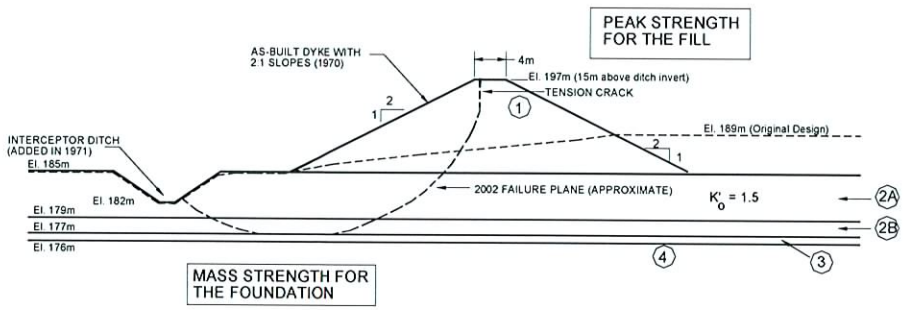

(b) With the interceptor ditch, 1971 (F.S. = 1.21)

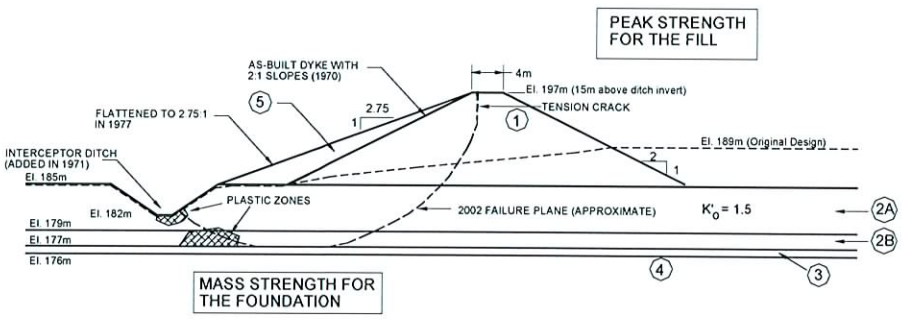

(c) After flattening the downstream slope (F.S. = 1.28)

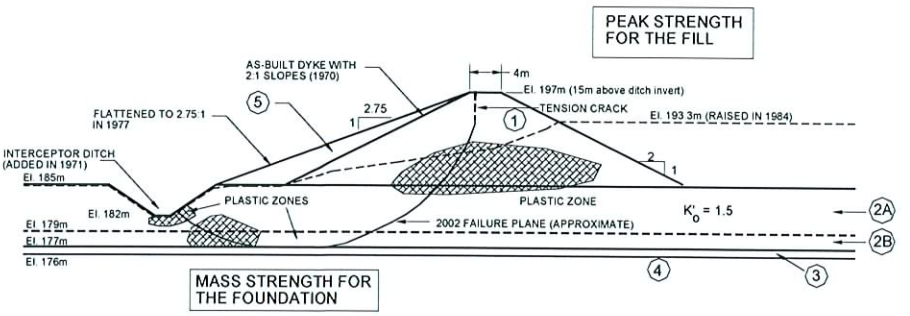

(d) After raising the pond level to el. 193.3m (F.S. = 1.20)

Figure 47. Zones of local failure after construction of the dyke and downstream interceptor ditch and at the normal headpond level

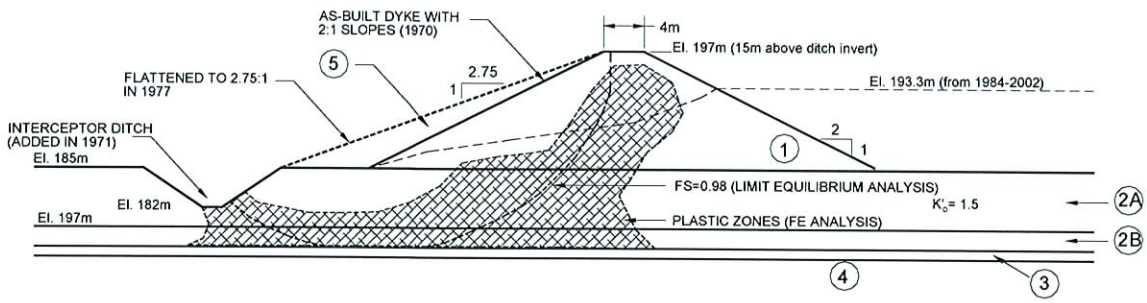

Figure 48. Zones of local failure using residual strength parameters for the geometry and operating condition from 1984 to 2002.

Figure 47b shows the impact of excavating the interceptor ditch in 1971 6m downstream of the dyke. For this condition, there are no zones of local failure in the dyke or the foundation. This is due primarily to the positive effect of the ditch, which caused a reduction of piezometric head in the dyke that counterbalanced the removal of material from downstream of the dyke. For this case, the calculated factor of safety of the dyke was 1.21, which is slightly lower than before excavating the ditch.

In 1977, the downstream slope of the dyke was flattened from 2:1 to 2.75:1. The calculated zones of local failure for this condition are plotted in Figure 47c. Based on the finite element calculations, it appears that flattening the downstream slope caused a stress concentration and a zone of local plasticity near the interceptor ditch. At this stage, the global factor of safety of the dyke increased to about 1.28 based on limit equilibrium analysis. Thus, a remedial measure that was implemented to control shallow slumping of the dyke fill caused a slight increase of the global factor of safety; However, the remedial measure also created a stress concentration near the downstream toe and interceptor ditch.

The third and final change to the dyke geometry and operation occurred in 1984 when the upstream pond level was raised to el. 193.3m. Figure 47d shows the resultant zones of local failure and the eventual failure surface for this condition. At the higher head pond level (el. 193.3m), there are extensive zones of local failure in the fill and the foundation. Over 40% of the critical slip surface has reached the peak strength of either the dyke or foundation materials. From limit equilibrium analysis, however, the global factor of safety was about 1.2, which at the time would probably not have caused major concern.

Based on the preceding results and discussions, it is concluded that changes to the Nanticoke dyke geometry and operating conditions had a significant impact on the state of effective stresses in the Nanticoke dyke and foundation. The impact of these changes did not and could not be reflected on the global factor of safety based on limit equilibrium analysis. The most significant change in the stress state occurred after raising the upstream pond level to el. 193.3m in 1984 resulting in significant zones of local failure in both the dyke and the foundation. With more than 40% of the potential failure plane reached the peak strength or mass strength of either the fill or foundation, respectively. Such stresses significantly exceed the residual strength of the dyke and foundation materials thereby inducing the potential for softening and decrease of strength from the peak or mass strength to the residual strength.

Figure 48 shows calculated zones of local failure based on the residual strength parameters of both the foundation and the fill materials (c_r'=13 kPa and ϕ_r'=15°). The critical slip surface obtained from limit equilibrium analysis is also plotted in Figure 48 for the conditions considered. Base on this analysis, zones of failure in the dyke and foundation are contiguous and the dyke is on the verge of collapse (e.g. the factor of safety is about 1). In addition, the extent and distribution of plastic zones from finite element analysis agree well with the results of limit equilibrium analysis. Thus, the analysis summarized in Figure 48 indicates that the residual strength of the Nanticoke fill and foundation was mobilized at the time of the 2002 failure. The time required for the failure to manifest was 32 years after construction and about 18 years after raising the level of the upstream pond.

9. CONCLUSIONS

This keynote address considers the implications of the macroscopic and microscopic structures of clays on the stability of earth structures. The microscopic structure consisting of the fabric and bonds of the clay particles was studied by a review of the behaviour of sensitive

clays, experiments with electrokinetic cementation and bonding in natural soils. The effects of macroscopic structure which is mainly constituted by fissures in stiff clays and in the crust of soft to firm clay deposits are examined using the results of field tests and previous case histories. Two recent case histories of failures, one in soft clay and one in stiff-fissured clay, were analyzed in detail so as to address some important issues relating to the capability to predict imminent instability using a conventional design method. From the results of this study, the following conclusions can be drawn:

(1) In sensitive clays, the concept of post-peak strength developed in the late 1960s and early 1970s which would allow for strength anisotropy time effects and progressive failure and is independent of stress paths remains valid. Design based on a post-peak envelope would implicitly account for the effects of microstructure.

(2) Electrokinetically-induced bonding tests showed that iron compounds, and Fe_2O_3 in particular, are effective bonding agents capable of increasing the strength, inducing brittleness and producing pseudo-overconsolidation, all in substantial amounts. An important mechanism of formation of bonding is ionic diffusion.

(3) Mineralogical studies showed that iron compounds are prevalent in Champlain Sea Clays both in the soft and very stiff sensitive clays, acting as an important bonding agent in these natural deposits.

(4) In clay deposits where fissuring is evident, it is important to appreciate the difference in strength of the intact material, along the fissures and the soil mass (operational strength). The strength of stiff fissured clays, whether in the undrained or drained state, decreases with an increase in sample size towards the mass strength in the field. Therefore, strength determined from conventional U-U tests on 50 mm samples would be on the unsafe side if directly used for design.

(5) Field evidence indicates that the fissured crust of soft to firm clay deposits showed similar behaviour as stiff-fissured clay. The strength in the crust measured by the field vane test is close to the intact strength and should therefore be reduced accordingly for the design of embankments on soft clay deposits.

(6) Results of analysis of the Vernon Embankments and Skå-Edeby Test Field emphasize the vast difference in behaviour between different loading geometries at the same surface loading. The key factor is the generation and extent of the plastic zone which delineates the region of damage to the microstructure of soft sensitive clays. Within the plastic zone, pore pressure increases at a rapid rate and may continue to rise at constant loading due to an increase in shearing strain causing further breakage. Propagation of the plastic zone to the ground surface led to collapse (Vernon Embankment). For stable embankments, no increase in strength with time results within the plastic zone for long periods (Skå-Edeby Embankment).

(7) As the critical height of the embankment is approached, the stability of the embankment is at a meta-stable state. The plastic zone increases in extent at small increments of loading or by progressive failure at constant loading. This state of behaviour cannot be reflected in limit equilibrium analysis. Appropriate finite element or similar stress analysis should be performed to delineate the details of foundation behaviour.

(8) The use of mass (operational) strength in terms of effective stress which accounts for the macrostructure of fissured clays appears to be able to capture the development of plastic zones caused by post-construction changes in geometric and groundwater conditions under long-term embankment loading.

(9) Analogous to conclusion (7) relevant to soft clays, factors of safety from limit equilibrium analysis cannot reflect subtle change in stability condition for embankments in stiff-fissured clays. For the evaluation of stability, the development of plastic zone due to minor changes in post-construction condition should be investigated.

It is suggested that relevant sections of the above conclusions may serve as additional design considerations for embankments on clay foundations.

10. ACKNOWLEDGEMENTS

The authors would like to acknowledge the work of Dr. Silvana Micic – Trow International and Messrs. Guangfeng Qu and Yi (George) Liang – Graduate Students at The University of Western Ontario. In addition, the research performed is supported by NSERC Discovery Grant 7745-03. Appreciation is expressed to Ontario Power Generation for the information on the Ash Disposal Dyke of Nanticoke G.S.

11. REFERENCES

Becker, D.E. (1981). Settlement analysis of intermittently-loaded structures founded on clay soils. PhD Thesis, Faculty of Engineering Science, University of Western Ontario.

Bieniawski, Z.T. (1968). The effect of specimen size on compressive strength of coal. Int. J. Rock Mech. Min. Sci., Vol. 5, pp. 325-335.

Bishop, A.W. and Little, A.L. (1967). The influence of the size and orientation of the sample on the apparent strength of the London Clay at Maldon, Essex. Proceedings Geotechnical Conference, Oslo 1, pp. 89-96.

Bjerrum, L. and Lo, K.Y. (1963). Effect of aging on the shear strength properties of a normally-consolidated clay. Geotechnique, Vol. 13, No. 2, pp. 147-157.

Bozozuk, M. and Leonards, G.A. (1972). The Gloucester Test Fill. Proceedings of Specialty Conference on

Performance of Earth and Earth-Supported Structures, ASCE, Purdue University, Vol. 1, pp. 299-317.

Carter, J.P. and Balaam, N.P. (1995). AFENA – A General Finite Element Algorithm: Users Manual. School of Civil Engineering and Mining Engineering, University of Sydney, N.S.W. 2006, Australia.

Casagrande, L. (1949). Electro-osmosis in soils. Geotechnique, Vol. 1, pp. 159-177.

Conlon, R. J. (1966). Landslide on the Toulnustouc River, Quebec. Canadian Geotechnical Journal, Vol. 3, No. 3, pp. 113-144.

Corbett, B.O. (1967). Discussion, Proceedings: Geotechnical Conference, Oslo, Norway, Vol. 2, pp. 161-165.

Crawford, C.B. (1963). Cohesion in an undisturbed sensitive clay. Geotechnique, Vol. 13, No. 2, pp. 132-146.

Crawford, C.B., Fannin, R.J., deBoer, L.J. and Kern, C.B. (1992). Experiences with prefabricated vertical (wick) drains at Vernon, B.C. Canadian Geotechnical Journal, Vol. 29, pp. 67-69.

Crawford, C.B., Fannin, R.J. and Kern, C.B. (1995). Embankment failures at Vernon, British Columbia. Canadian Geotechnical Journal, Vol. 32, No. 2, pp. 271-284.

Daniel, D.E. and Olson, R.E. (1982). Failure of an anchored bulkhead. Journal of the Geotechnical Engineering Division, Proc. ASCE, Vol. 108, No. GT10, pp. 1318-1327.

Dascal, O., Tournier, J.P., Tavenas, F. and La Rochelle, P. (1972). "Failure of test embankment on sensitive clay." Proceedings, ASCE Specialty Conference on Performance of Earth and Earth-Supported Structures. Purdue University, Lafayette, IN, Vol. 1, pp. 129-158.

Dixon, J.B., Weed, S.B., Kittrick, J.A., Milford, M.H. and While, J.L. (1977). Minerals in soil environments. Soil Science Society of America, pp. 145-176.

Graham, J. (2003). The R.M. Hardy Address: Soil parameters for numerical analysis in clays. Proceedings 56th Canadian Geotechnical Conference, Winnipeg, Manitoba, September.

Hardy, R.M., Brooker, E.W. and Curtis, W.E. (1962). Landslides in over-consolidated calys. Engineering Journal, 45(1), pp. 81-89.

Holtz, R.D. and Broms, B. (1972). Long-term loading tests at Skå-Edeby, Sweden. Proceedings of the ASCE Specialty Conference on the Performance of Earth-Supported Structures, Purdue University, Lafayette, Indiana, pp. 435-464.

Holtz, R.D. and Lindskog, G. (1972). Soil movement below a test embankment. Proceedings of the ASCE Specialty Conference on the Performance of Earth-Supported Structures, Purdue University, Lafayette, Indiana, pp. 273-284.

Kenney, T.C., Moum, J., and Berre, T. (1967). An experimental study of bonds in a natural clay. Proceedings Geotechnical Conference, Oslo 1, pp. 65-69.

Kuluk, A.G. (1974). Private communications (describing subsequent movements after Peterson et al. 1960 paper).

La Rochelle, P. and Lefebvre, G. (1971). Sampling disturbance in Champlain clays. American Society for Testing and Materials, Special Technical Publication 483, pp. 143-163.

La Rochelle, P., Trak, B., Tavenas, F. and Roy, M. (1974). Failure of a test embankment on a sensitive Champlain clay deposit. Canadian Geotechnical Journal, 11, pp. 142-164.

Law, K.T. (1975). Analysis of embankments on sensitive clays. PhD. Thesis, Faculty of Engineering Science, University of Western Ontario.

Law, K.T. (1981). Effect of stress path geometry on soil brittleness. Geotechnique, Vol. 31, No. 2, pp. 279-287.

Lefebvre, G. (1981). Strength and slope stability in Canadian soft clay deposits. Fourth Canadian Geotechnical Colloquium, Vol. 18, No. 3, pp. 420-442.

Lefebvre, G. and La Rochelle, P. (1974). The analysis of two slope failures in cemented Champlain clays. Canadian Geotechnical Journal, 2, pp. 89-108.

Lefebvre, G., Paré, I.J. and Dascal, O. (1987). Undrained shear strength in surficial weathered crust. Canadian Geotechnical Journal, Vol. 24, pp. 23-34.

Leonards, G.A. and Ramiah, B.K. (1959). Time effect in the consolidation of clays. American Society for Testing Materials, Special technical publication, 254, pp. 116-130.

Leroueil, S. (2005). Clay behaviour and mobilized strength in clay slopes. Proceedings of K.Y. Lo Symposium, Geotechnical Research Centre, University of Western Ontario.

Leroueil, S. and Vaughan, P.R. (1990). The general and congruent effects of structures in natural soils and weak rock. Geotechnique, Vol. 40, pp. 467-488.

Liang, Y. (2006). Progressive failure of the Nanticoke Ash Lagoon Dyke. M.E.Sc. Thesis, The University of Western Ontario.

Lo, K.Y. (1961). Stress-strain relationship and pore water pressure characteristics of a normally-consolidated clay. Proceedings Fifth International Conference on Soil

Mechanics and Foundation Engineering, Paris, July 17-22, Vol. I, pp. 219-224.

Lo, K.Y. (1970). The operational strength of fissured clays. Geotechnique, Vol. 20, No. 1, pp. 57-74.

Lo, K.Y. (1972). An approach to the problem of progressive failure. Canadian Geotechnical Journal, Vol. 9, No. 4, pp. 407-429.

Lo, K.Y. (1973). Behaviour of embankment on sensitive clays loaded close to failure. Report to Ontario Department of Highways. SM-2a-73, Faculty of Engineering Science, The University of Western Ontario, August.

Lo, K.Y. and Ho, K.S. (1991). Electroosmotic strengthening of soft sensitive clays. Canadian Geotechnical Journal, No. 28, pp. 62-73.

Lo, K.Y. and Lee, C.F. (1974). An evaluation of the stability of natural slopes in plastic Champlain clays. Canadian Geotechnical Journal, Vol. 11, No. 1, pp. 165-181.

Lo, K.Y. and Morin, J.P. (1972). Strength anisotropy and time effects of two sensitive clays. Canadian Geotechnical Journal, Vol. 9, No. 3, pp. 261-277.

Lo, K.Y. and Vallee, J. (1970). Strength anisotropy due to parallel planes of discontinuities in clays. Proceedings Second Southeast Asian Conference on Soil Engineering, Singapore, pp. 245-263.

Lo, K.Y., Adams, J.I. and Seychuk, J.L. (1969). The shear behaviour of a stiff fissured clay. Proceedings Seventh International Conference on Soil Mechanics and Foundation Engineering, Mexico, Vol. I, pp. 249-255.

Man, A., Graham, J., Alfaro, M. and Goh, T.B. (2003). Changes in clay behaviour produced by seepage under a water retention dyke. Proceedings 56th Canadian Geotechnical Conference, Winnipeg, Manitoba, September.

Marsland, A. and Butler, M.E. (1967). Strength measurements on stiff fissured Barton Clay from Fawley, Hampshire. Proceedings Geotechnical Conference, Oslo 1, pp. 139-145.

Micic, S., Shang, J.Q. and Lo, K.Y. (2002). Electrokinetic strengthening of marine clay adjacent to offshore foundations. International Journal of Offshore and Polar Engineering, 12(1), pp. 64-73.

Mitchell, J.K. (1976). Fundamentals of Soil Behaviour. John Wiley & Sons Inc.

Mitchell, J.K. and Wan, T.Y. (1977). Electro-osmotic consolidation – its effects on soft soils. Proceedings 9th International Conference on Soil Mechanics and Foundation Engineering, Tokyo, Vol. 1, pp. 219-224.

Morin, J.P. (1975). Geotechnical behaviour of two quaternary clays from the central St. Lawrence lowland. Ph.D. Thesis, Laval University.

Ohtsuki, H., Nishi, K. Okamoto, T. and Tanaka, S. (1981). Time dependent characteristics of strength and deformation of mudstone. Proceedings: Symposium on Weak Rock, Tokyo, Japan, Vol. 1, pp. 119-124.

Peterson, R., Jaspar, J.L., Rivard, P.J. and Iverson, N.L. (1960). Limitations of laboratory shear strength in evaluating stability of highly plastic clays. Res. Conf. Shear Strength Cohesive Soils, Boulder, American Society of Civil Engineers, pp. 765-791.

Quigley, R.M. (1968). Landslide on the Toulnustouc River, Quebec: Discussion. Canadian Geotechnical Journal, 3, pp. 175-177.

Quigley, R.M. and Ogunbadejo, T.A. (1972). Clay layer fabric and oedometer consolidation of a soft varved clay. Canadian Geotechnical Journal, 9, pp. 165-175.

Quigley, R.M. and Thompson, C.D. (1966). The fabric of anisotropically consolidated sensitive marine clays. Canadian Geotechnical Journal, Vol. 3, No. 2, pp. 61-73.

Quigley, R.M. (1980). Geology, mineralogy, and geochemistry of Canadian soft soils: a geotechnical perspective. Canadian Geotechnical Journal, Vol. 17(2), pp. 261-285.

Rosenqvist, I.T. (1966). Norwegian research into the properties of quick clay – a review. Engineering Geology, 1, pp. 445-450.

Simons, N.E. (1967). Discussion on shear strength of stiff clay. Proceedings Geotechnical Conference, Oslo 2, pp. 159-160.

Skempton, A.W. (1977). Slope stability of cuttings in brown London clay. Proceedings, IX International Conference SMFE (Tokyo), Vol. 3, pp. 261-270.

Skempton, A.W. and La Rochelle, P. (1965). The Bradwell slip: a short-term failure in London Clay. Geotechnique, Vol. 15, No. 3, pp. 221-241.

Skempton, A.W. and Petley, D.J. (1967). The strength along structural discontinuities in stiff clays. Proceedings Geotechnical Conference, Oslo 2, pp. 29-46.

Skempton, A.W., Schuster, R.L. and Petley, D.J. (1969). Joints and fissures in the London Clay at Wraysbury and Edgware. Geotechnique, 19 No. 2, pp. 205-217.

Trak, B., La Rochelle, P., Tavenas, F. and Leroueil, S. (1980). A new approach to the stability analysis of embankments on sensitive clays. Canadian Geotechnical Journal, Vol. 17, pp. 526-543.

Vallée, J. (1969). The influence of fissures on the shear behaviour of a stiff clay. MESc Thesis, Dept. of Civil Engineering, Laval University.

Yong, R.N., Sethi, A.J. and La Rochelle, P. (1979). Significance of amorphous material relative to sensitivity in some Champlain clays. Canadian Geotechnical Journal, 16, pp. 511-520.